LA-8741-MS
NUREG/CR-1991

TRAC-PD2 Posttest Analysis of CCTF Test C1-16 (Run 025)

University of California

LOS ALAMOS SCIENTIFIC LABORATORY
Post Office Box 1663 Los Alamos, New Mexico 87545

An Affirmative Action/Equal Opportunity Employer

NUREG/CR-1991
LA-8741-MS
R4

TRAC-PD2 Posttest Analysis of CCTF Test C1-16 (Run 025)

J. Sugimoto*

Manuscript submitted: February 1981
Date published: May 1981

Prepared for
Division of Reactor Safety Research
Office of Nuclear Regulatory Research
US Nuclear Regulatory Commission
Washington, DC 20555

and Japan Atomic Energy Research Institute
Tokai-Mura, Naka-Gun, Ibaraki-Ken JAPAN

NRC FIN No. A7049

*Visiting Scientist. Japan Atomic Energy Research Institute, Tokai-Mura, Naka-Gun, Ibaraki-Ken, JAPAN.

UNITED STATES
DEPARTMENT OF ENERGY
CONTRACT W-7405-ENG. 36

TRAC-PD2 POSTTEST ANALYSIS OF CCTF TEST C1-16 (RUN 025)

by

J. Sugimoto

ABSTRACT

The TRAC-PD2 code version was used to analyze CCTF Test C1-16 (Run 025). The results indicate that the core heater rod temperatures, the liquid mass in the vessel, and differential pressures in the primary loop are predicted well, but the void fraction distribution in the core and water accumulation in the upper plenum are not in good agreement with the data.

I. INTRODUCTION

This paper summarizes the modeling and selected results from the TRAC-PD2 posttest analysis of the Cylindrical Core Test Facility (CCTF) experiment denoted C1-16 (Run 025). This test is a FLECHT coupling test based on initial conditions taken from FLECHT Test 3105B. The description of the CCTF facility and the experimental operating specifications were obtained from K. Hirano of the Japan Atomic Energy Research Institute. The TRAC version used for these calculations was a released version of TRAC-PD2[1] with no modifications.

II. DESCRIPTION OF THE TRAC-PD2 MODEL

The Transient Reactor Analysis Code (TRAC) input model nodalization is shown in Fig. 1. The input model consists of 18 components that are described in Table I. The total number of cells was 109. The input model was based primarily on the input model for a previous CCTF posttest analysis.[2] From this input model some renoding was performed; in particular, Vessel Level 3, in the

lower plenum, was converted to two levels, the core was converted from five levels to six, and the upper plenum was converted from one level to three.

The three intact loops containing the steam generators, pump simulators, and Emergency Core Cooling System (ECCS) injection ports were combined into a single loop as shown in Fig. 1. The pump simulators were modeled with PIPE components, which allowed a method of setting the pump orifice flow-resistance coefficient to the same value as used in the experiments.

A detailed noding schematic of the vessel component is shown in Fig. 2. The entire test vessel was subdivided into 52 vessel nodes, which allowed direct correspondence to actual differential pressure measuring points in the core. The coarse noding of the core region (six axial levels) required averaging of the CCTF axial power profile as shown in Fig. 3. It should be noted that the local power where thermocouples are located (elevations 3, 4, and 5) is almost identical to that of the experiments.

The heater rods were segmented into nine radial nodes, as shown in Fig. 4. TRAC doesn't currently model the material properties for aluminum oxide and magnesium oxide, which are the insulating materials in the CCTF heater rods. Instead, TRAC models boron nitride (BN) only, which was used in the calculation. (BN is also used for the central region of the actual heater rods in CCTF.)

III. INITIAL AND BOUNDARY CONDITIONS FOR CCTF C1-16 (RUN 025)

The initial test conditions used for the posttest analysis are tabulated in Table II. These test conditions and boundary conditions were taken from the experimental data, as reported by K. Harano. The sequence of events is summarized in Table III. All trips were made according to the actual sequence in the experiment. The hydraulic boundary conditions for the TRAC calculation were (1) the constant system pressure at two breaks in the cold leg and (2) the ECCS flow velocity at lower plenum injection fill (see Fig. 1). Figure 5 shows the comparison of the ECCS mass flow rate.

IV. DISCUSSION OF POSTTEST CALCULATIONAL RESULTS

The TRAC calculation was carried out to 317 s. The sequence of events is summarized in Table III. Heater rod temperature histories at five axial locations are compared to data (22Y1 rod) in Figs. 6 through 10. Data are shown in dotted lines. The calculations are in fairly good agreement with the

data, especially for the quench time, the quench temperature, and the turnaround temperature, except for the Z = 5.15 m elevation. TRAC tends to overpredict slightly the quench temperature for the upper part of the core. Void fractions in the core are sh wn in Figs. 11-16. The TRAC predictions are in good agreement with the data for the lower region of the core, but TRAC tends to overpredict the void fractions for the upper region. Although the void fraction data are directly converted from the differential pressure measurements, neglecting the frictional loss, the discrepancy between the two for the upper region is significant and requires further study.

The core inlet mass velocity is shown in Fig. 17. The TRAC calculation shows very large inlet flow oscillations. Core inlet mass velocity data were obtained by a mass balance calculation, using differential pressure measurements in the core and upper plenum and Pitot tube mass flow measurement in the cold legs; so it is difficult for the data to follow the high-frequency oscillations. The core inlet liquid temperature in Fig. 18 also reflects TRAC's prediction of a much higher temperature. The same overprediction also can be seen in Fig. 6 for the cladding temperature after quenching. This probably is due to the large calculated inlet flow oscillations, which cause considerable mixing of the water in the lower plenum, core, and downcomer.

The core liquid mass is shown in Fig. 19. The data were converted from the differential pressure measurement. The calculation agrees qualitatively well with the data. The underprediction of the core liquid mass is due to the higher void fractions in the upper part of the core. The downcomer liquid mass is shown in Fig. 20. The calculation is in good agreement with the data. As the downcomer wall was not heated above the saturation temperature in the experiment, this means that TRAC correctly calculates the rate of the water filling of the cold downcomer. The slight overprediction of the downcomer liquid at the overflowing level seems to be due to the effect of the downcomer-bypass phenomenon. Significant water overflow to the break was observed in CCTF before the time when the downcomer liquid level reaches the lower edge of the cold leg nozzles. Fairly large oscillations are seen in both core and downcomer liquid mass. These are out of phase with each other, causing essentially a U-tube type oscillation. The calculated amplitude of the oscillation is much larger than the experiment because the noding used in this analysis is of a one-dimensional nature.

The differential pressure in the upper plenum is shown in Fig. 21. The calculation shows very little water accumulation in the upper plenum, whereas the data show significant water formation due to carry-over water from core and de-entrainment in the upper plenum. This process was visually observed in the CCTF experiments. As TRAC calculated little carry over and the current version of TRAC does not assure the de-entrainment phenomena, the situation in the upper plenum seems to be much different qualitatively.

The fluid temperatures in the upper plenum are shown in Fig. 22. The data, measured at the hot leg nozzle elevation in the upper plenum, agree quite well with the calculated liquid temperature, but these data do not agree with the calculated vapor temperature. This means that the fluid in the upper plenum forms almost a saturated two-phase flow due to the presence of much water above the upper core support plate. The calculated vapor temperature, however, shows a superheated steam caused by the higher void fractions in the upper part of the core and in the upper plenum.

Figure 23 compares the absolute pressure in the upper plenum. The calculation shows a very large pressure spike when accumulator water is injected. After accumulator injection ended and low-pressure coolant injection (LPCI) was initiated, the pressure history agreed well with the data. The large pressure spike seems to be due to the large condensation rate in the core and lower plenum and may be a result of the one-dimensional noding in the vessel. A sensitivity study of a reduced condensation rate, added frictional loss, and/or three-dimensional noding in vessel would be needed to evaluate the large pressure spike. However, the effect of the pressure spike is not dominant, because the duration time is relatively short.

Differential pressures across the steam generator in the broken and intact loops are shown in Figs. 24-25. Differential pressures across the pump orifice are shown in Figs. 26-27. The calculations are in fairly good agreement with the data on the average. However, TRAC tends to underpredict slightly the broken loop values, and to overpredict for the intact loop. This implies that TRAC predicts a smaller flow resistance at the upper part of the downcomer as a downcomer-bypass flow restriction. The calculation shows larger and more regular oscillations for the intact loop than for the broken loop. This implies that U-tube oscillations in the calculation are caused and induced by the steady condensation at the upper part of the downcomer, near the intact cold leg.

V. CONCLUSIONS

The results of this TRAC-PD2 posttest analysis of CCTF Test C1-16 indicate that

1. TRAC predicts the heater rod temperature histories reasonably well as compared to the data;
2. the calculated void fractions are in good agreement for the lower region of core but in poor agreement for the upper region;
3. the calculated inlet water temperature is higher than the data due to large inlet flow oscillations;
4. the calculated liquid mass in the core and in the downcomer are in good agreement with the data;
5. TRAC does not predict the water accumulation in the upper plenum;
6. calculated average differential pressures across the steam generator and pump simulator are in reasonable agreement with the data;
7. a large pressure spike during the accumulator injection period is calculated, but it is dampened soon; and
8. sensitivity studies on the condensation rate, the additional friction loss, three-dimensional noding in the core, and downcomer-bypass flow resistance will be necessary.

ACKNOWLEDGMENTS

The author would like to thank W. Kirchner, K. Williams, R. Fujita, and T. Brown for their helpful advice and valuable discussions during this study.

REFERENCES

1. Safety Code Development Group, Energy Division, "TRAC-PD2, An Advanced Best-Estimate Computer Program for Pressurized Water Reactor Loss-of-Coolant Accident Analysis," Los Alamos National Laboratory report LA-8709-MS (May 1981).

2. R. K. Fujita, J. R. Ireland, and J. L. Elliott, "TRAC Posttest Prediction of CCTF Test C1-16 (Run 025)," 2D/3D Program Coordination Meeting, Tokai, Japan, March 3-7, 1980.

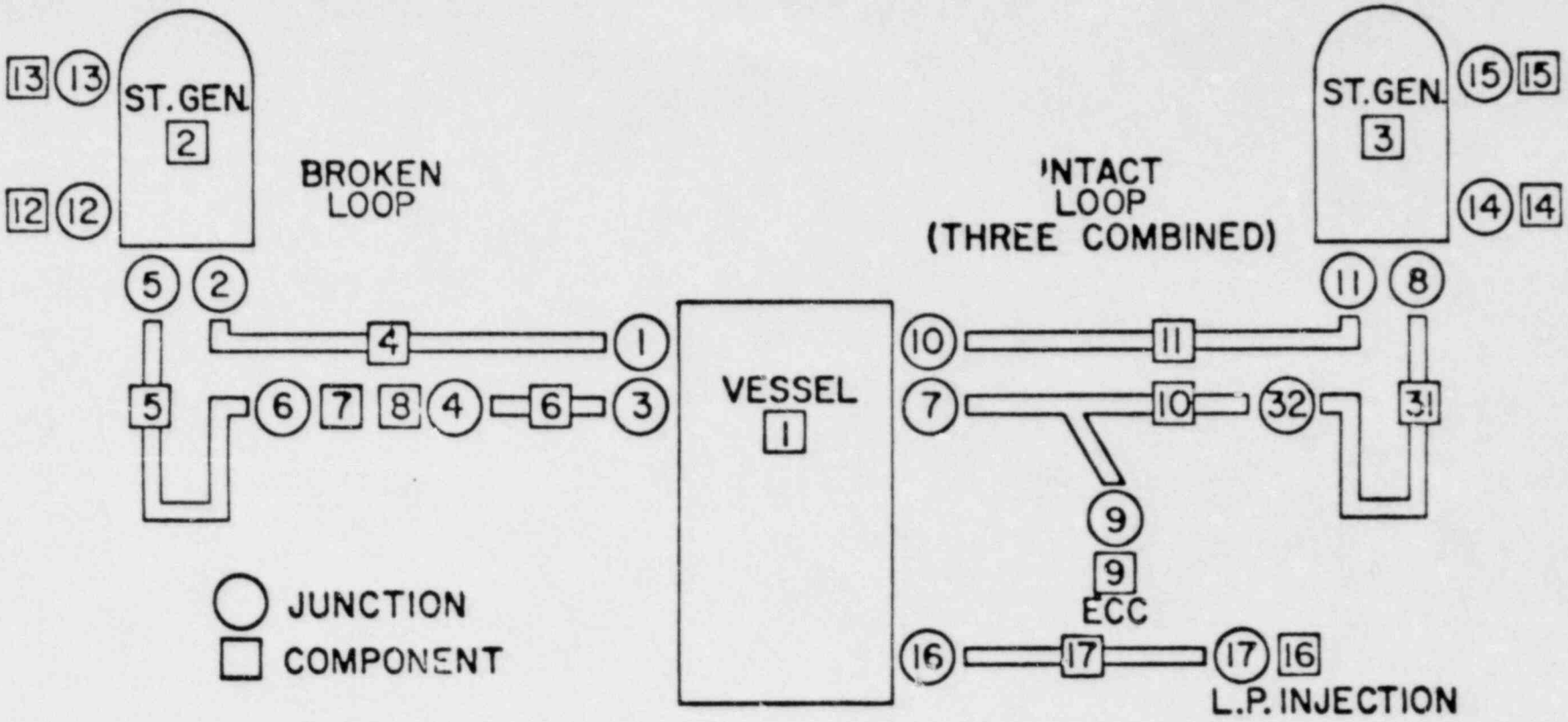

Fig. 1. TRAC component schematic.

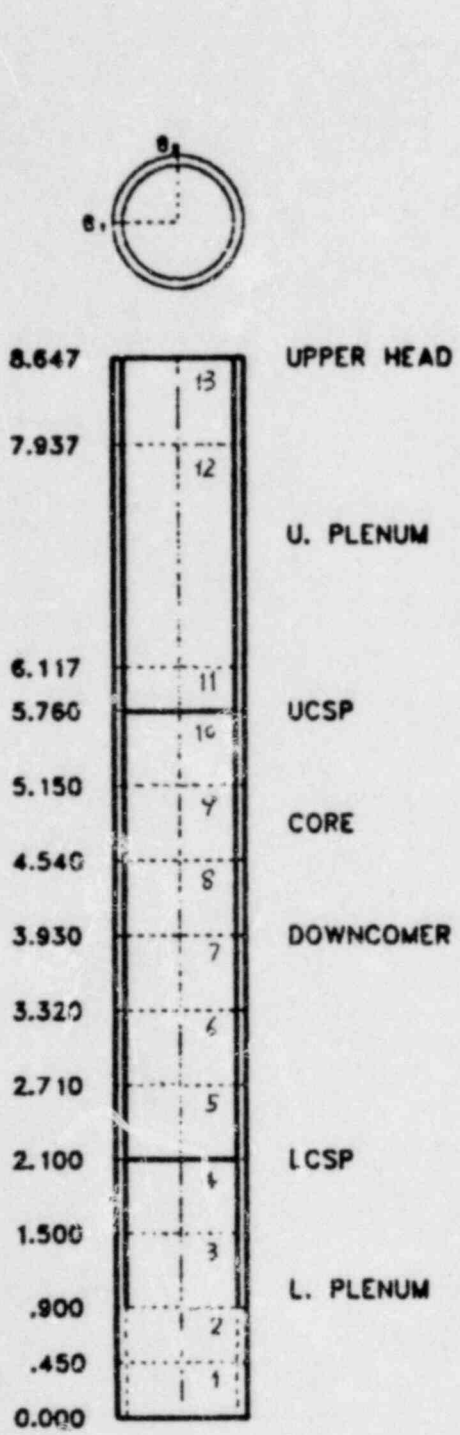

Fig. 2. Vessel noding.

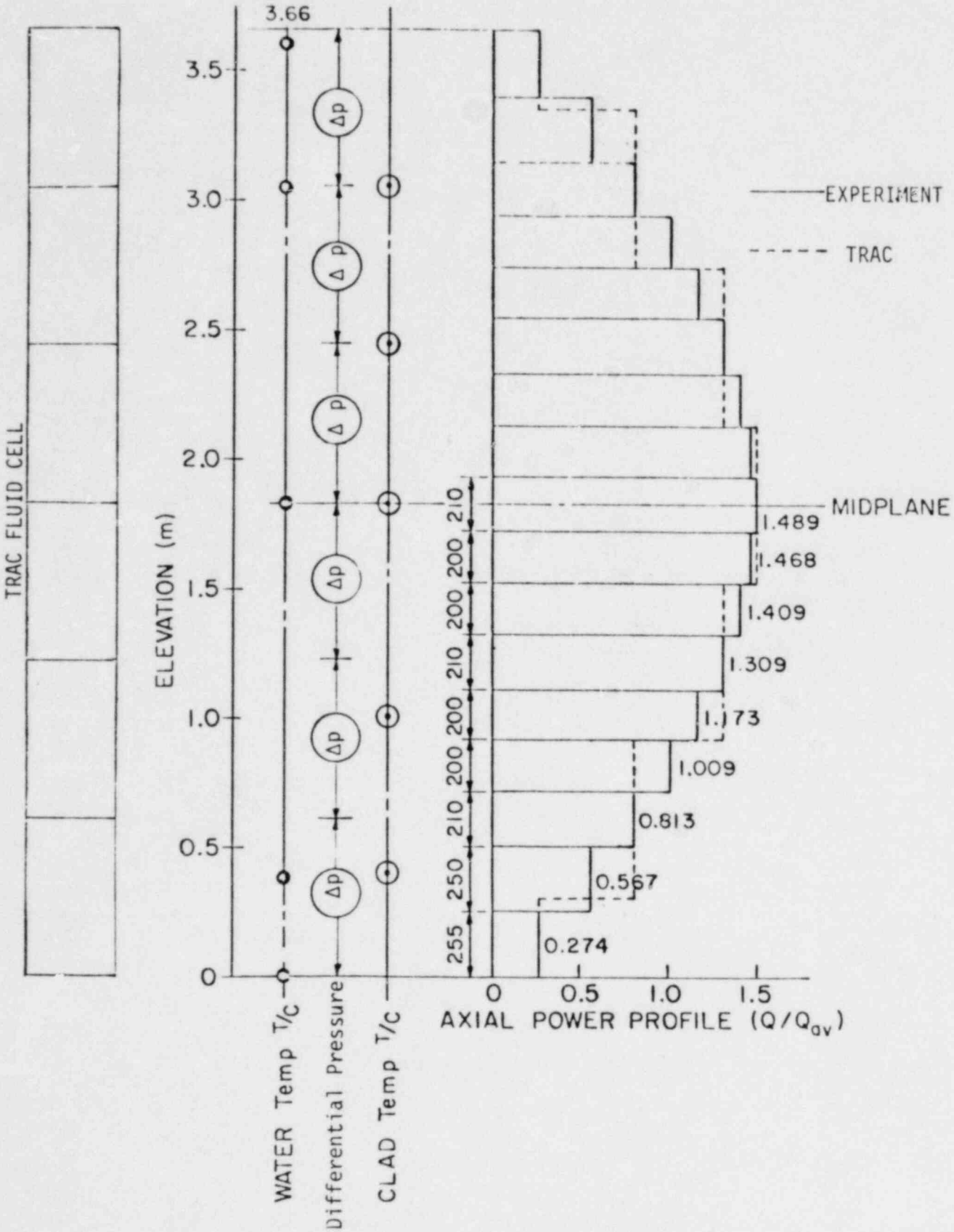

Fig. 3. Axial power profile.

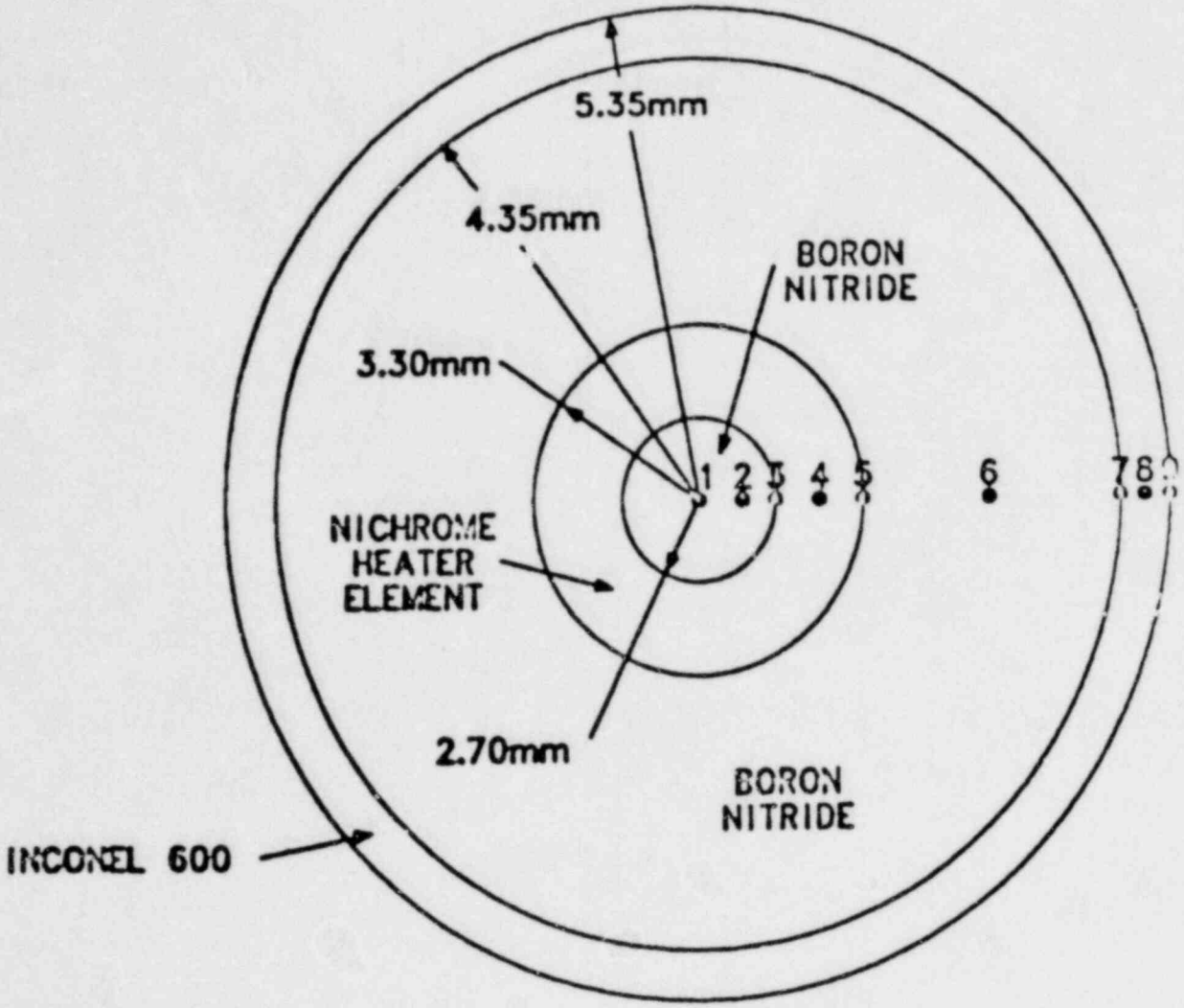

Fig. 4. Heater rod noding.

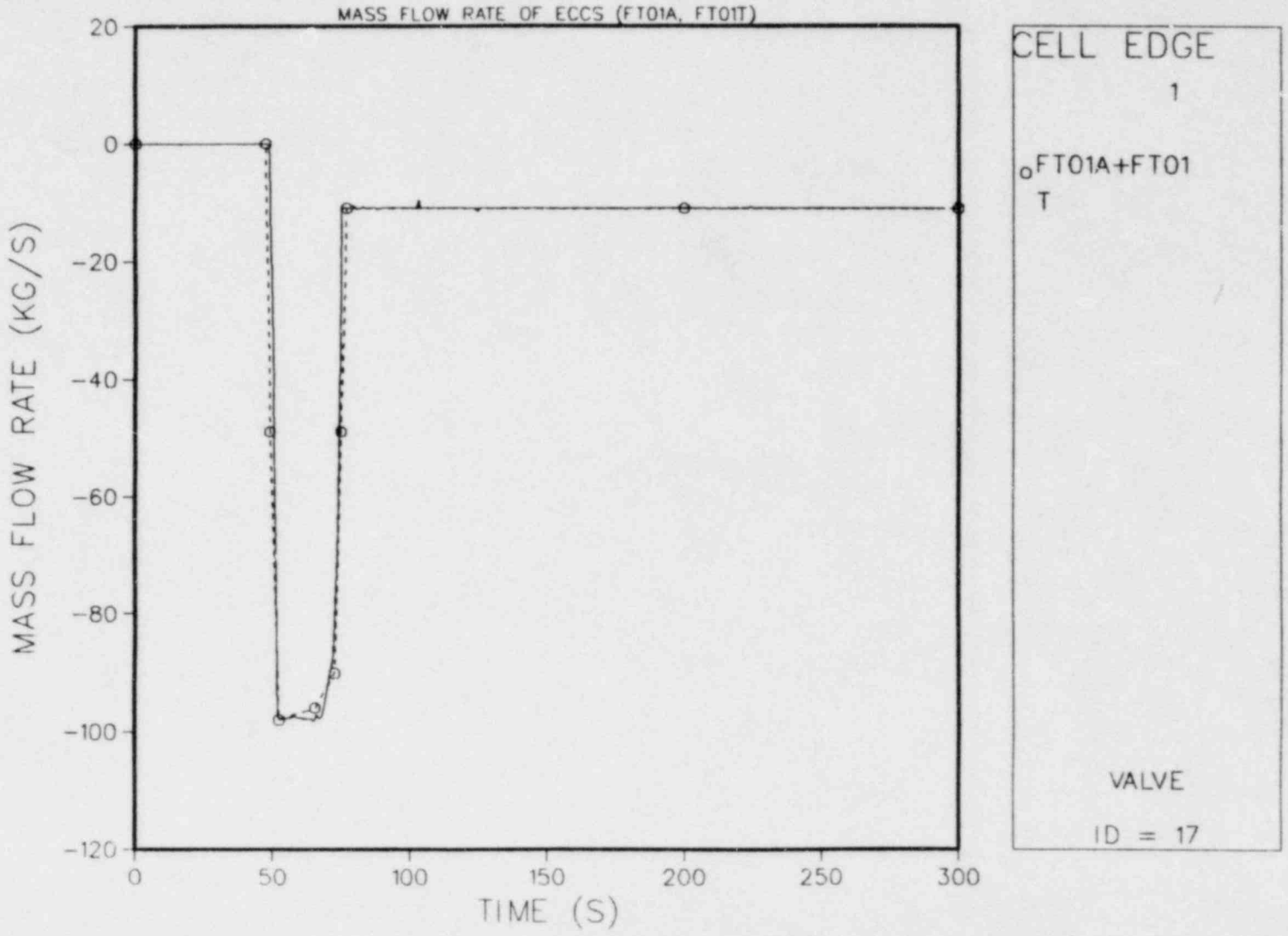

Fig. 5. ECCS mass flow rate.

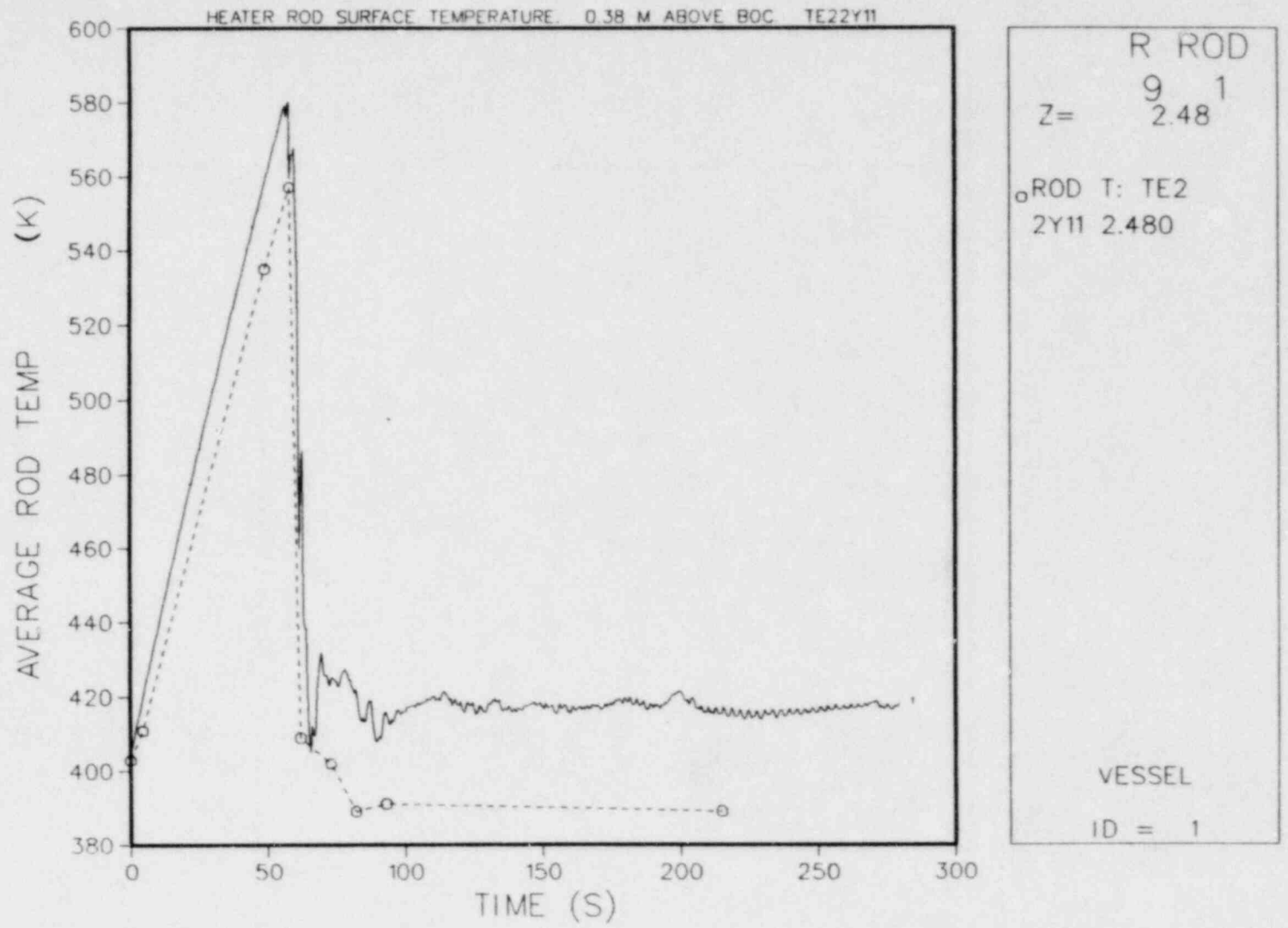

Fig. 6. Rod temperature at 2.48 m.

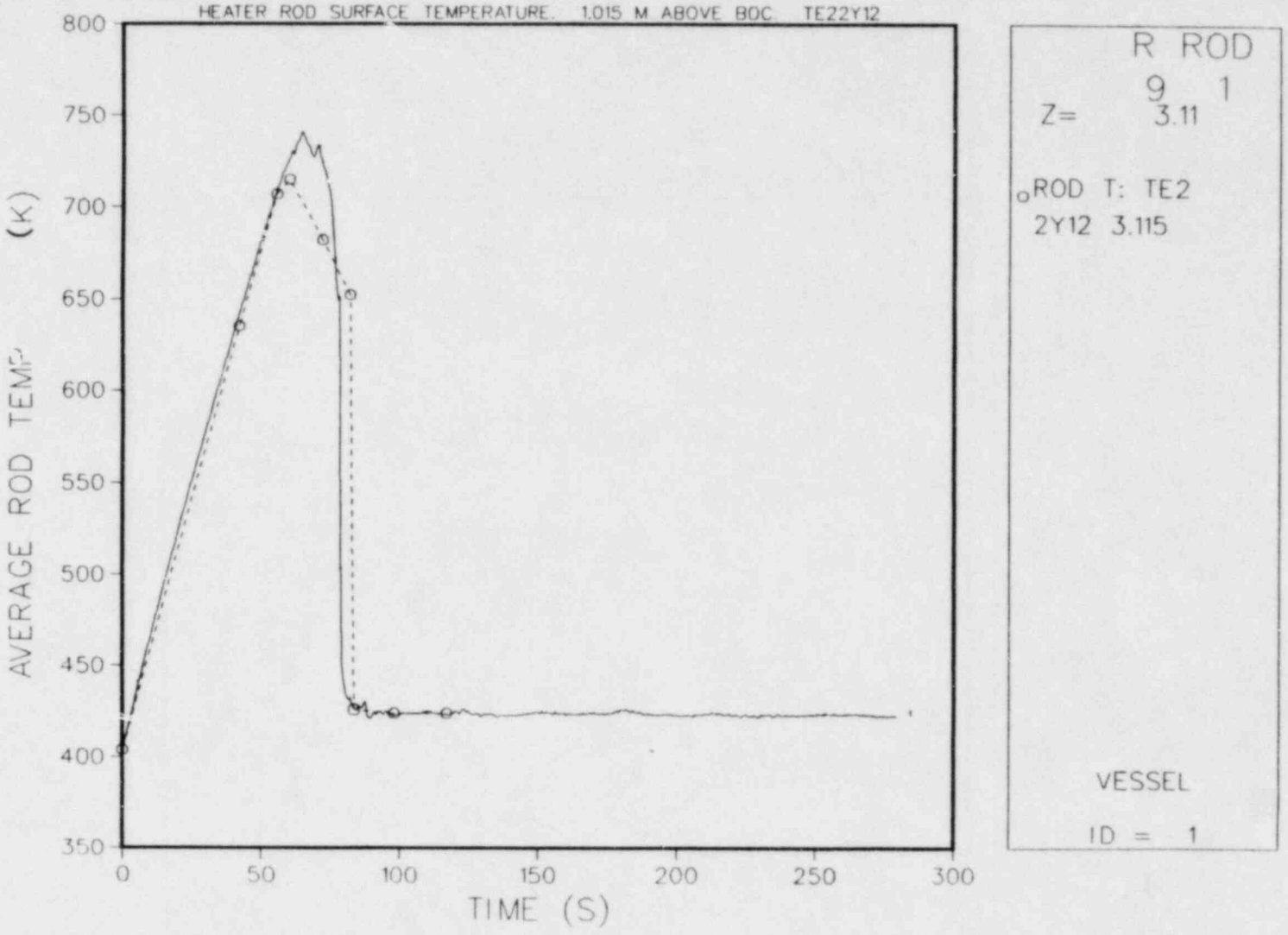

Fig. 7. Rod temperature at 3.115 m.

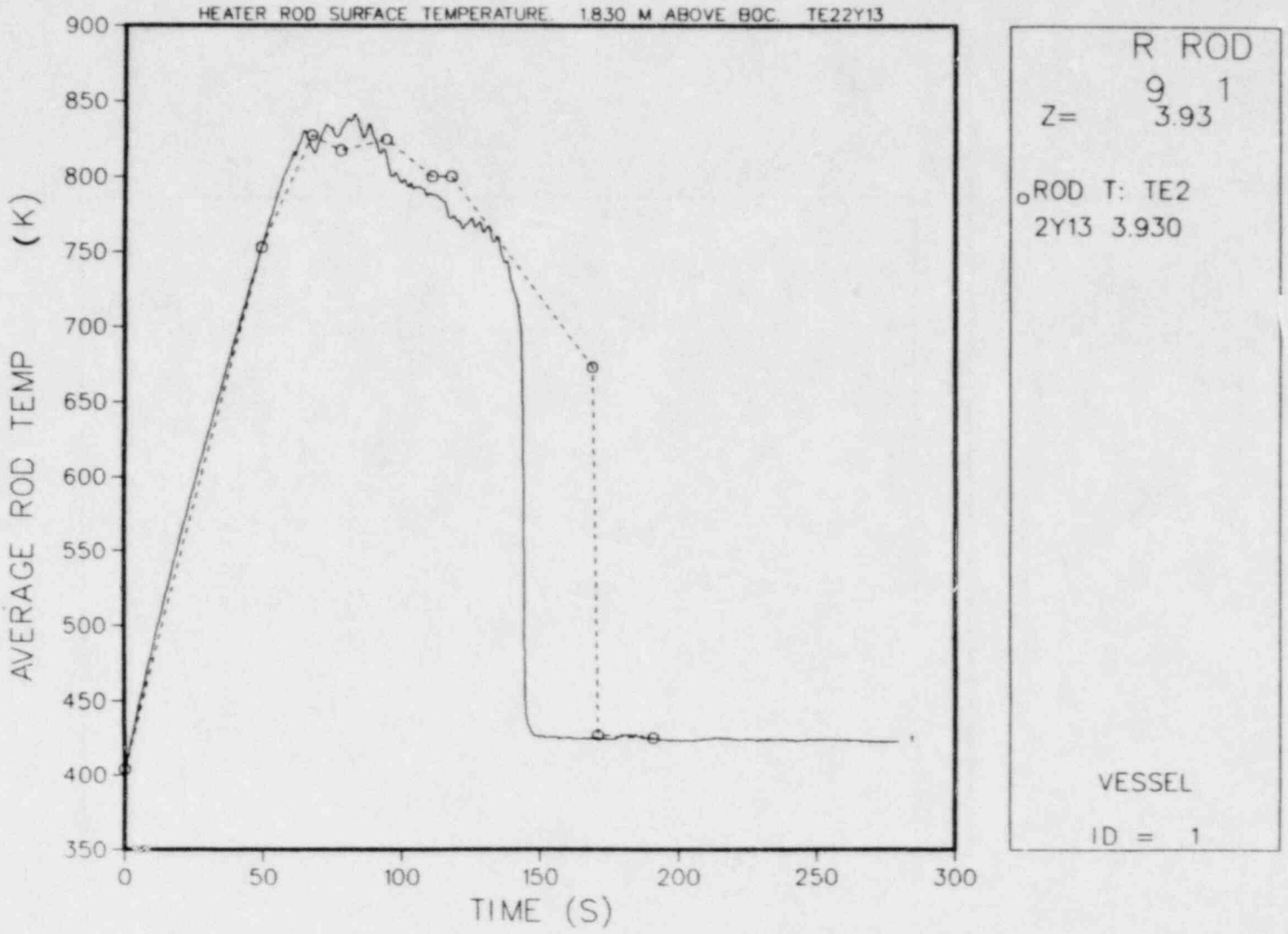

Fig. 8. Rod temperature at 3.93 m.

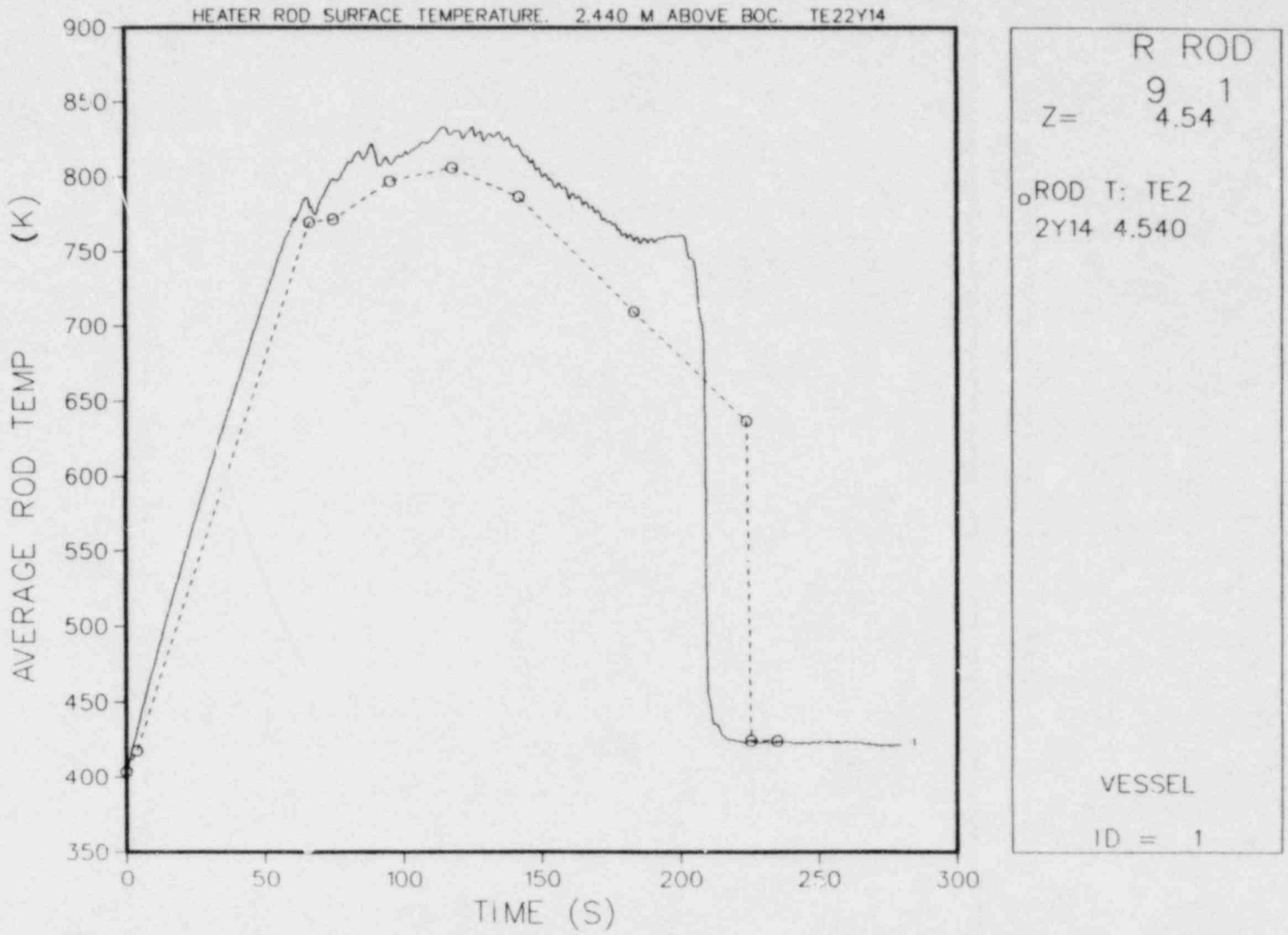

Fig. 9. Rod temperature at 4.54 m.

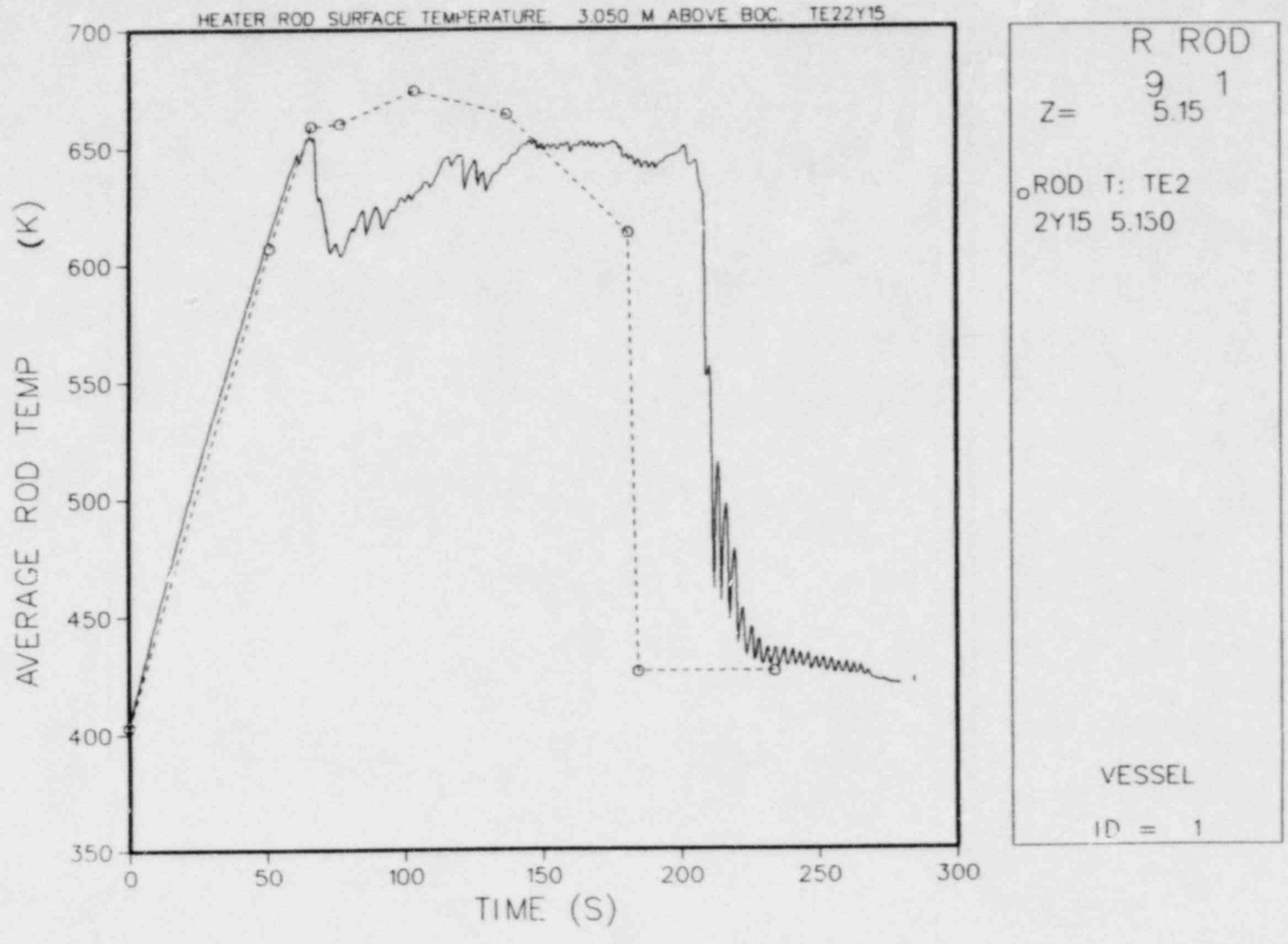

Fig. 10. Rod temperature at 5.15 m.

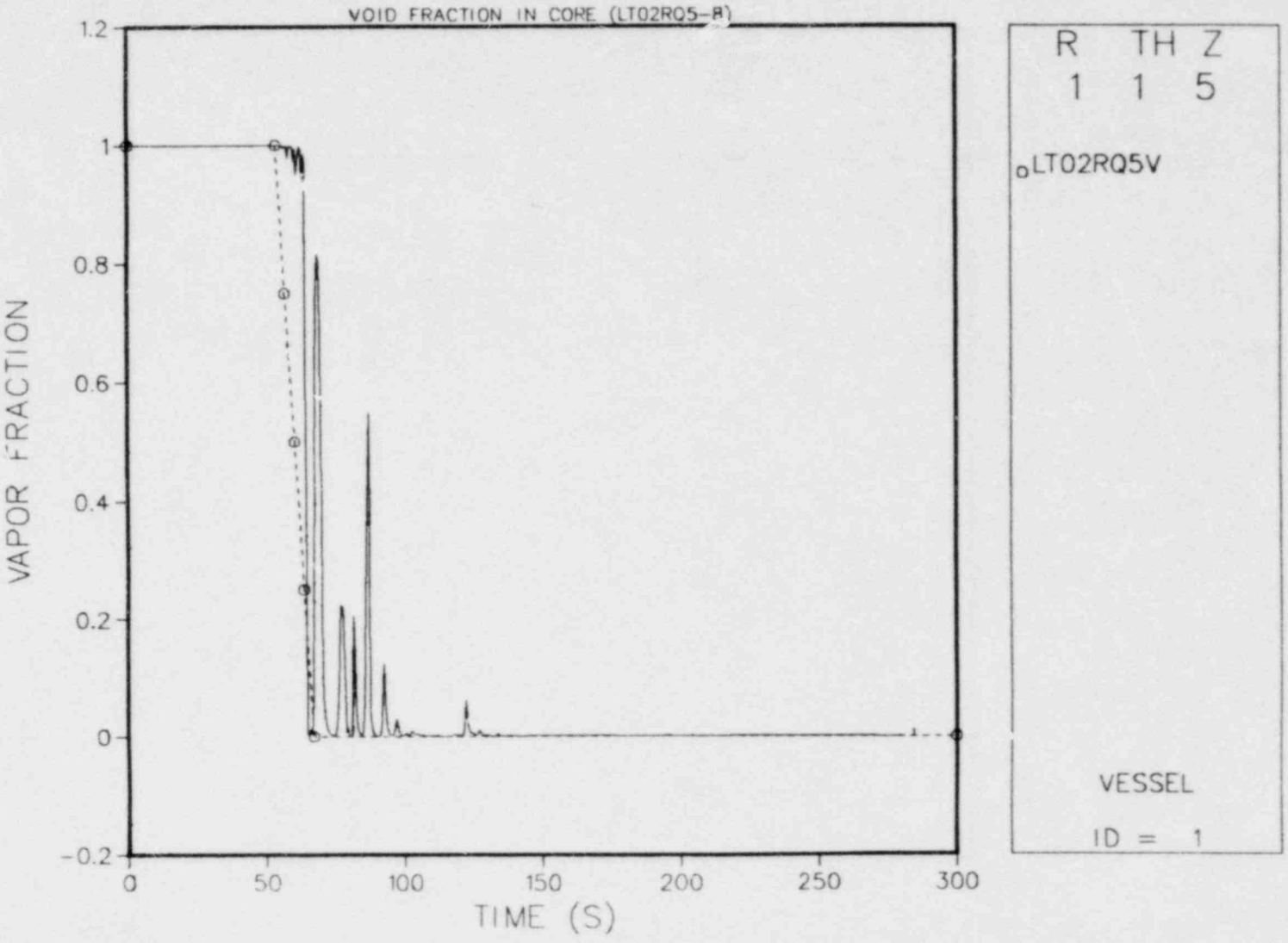

Fig. 11. Void fraction in core (Level 5).

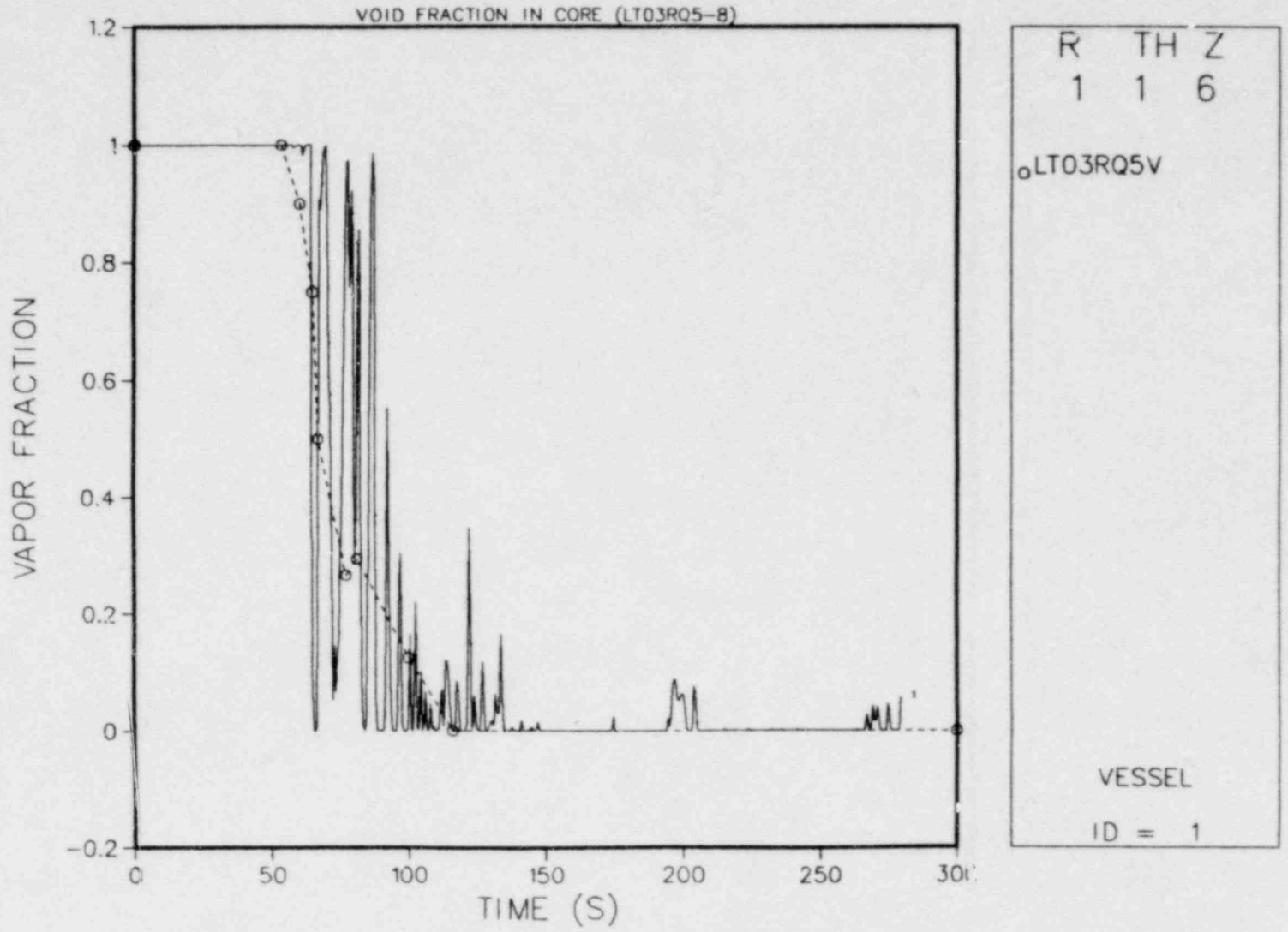

Fig. 12. Void fraction in core (Level 6).

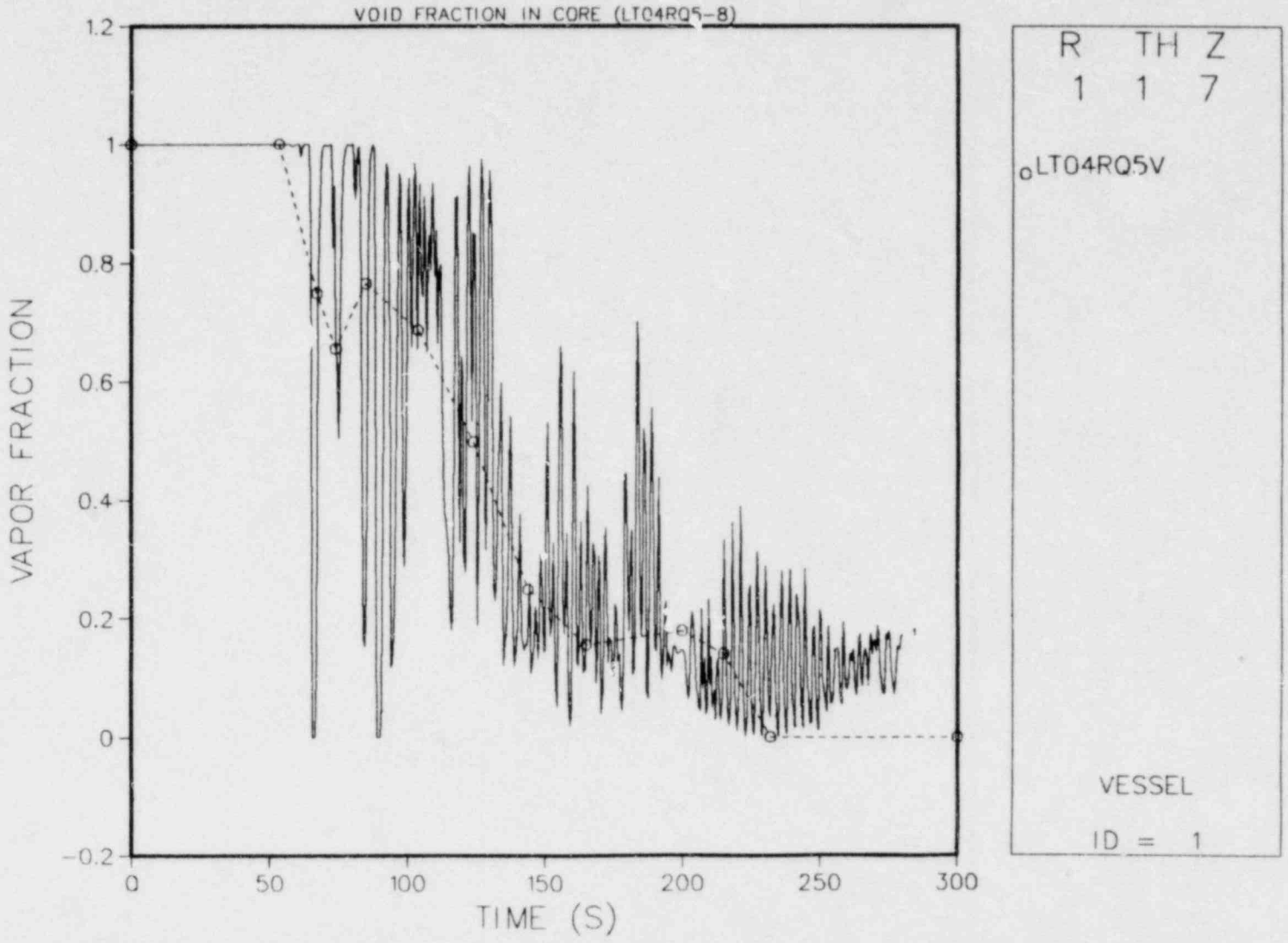

Fig. 13. Void fraction in core (Level 7).

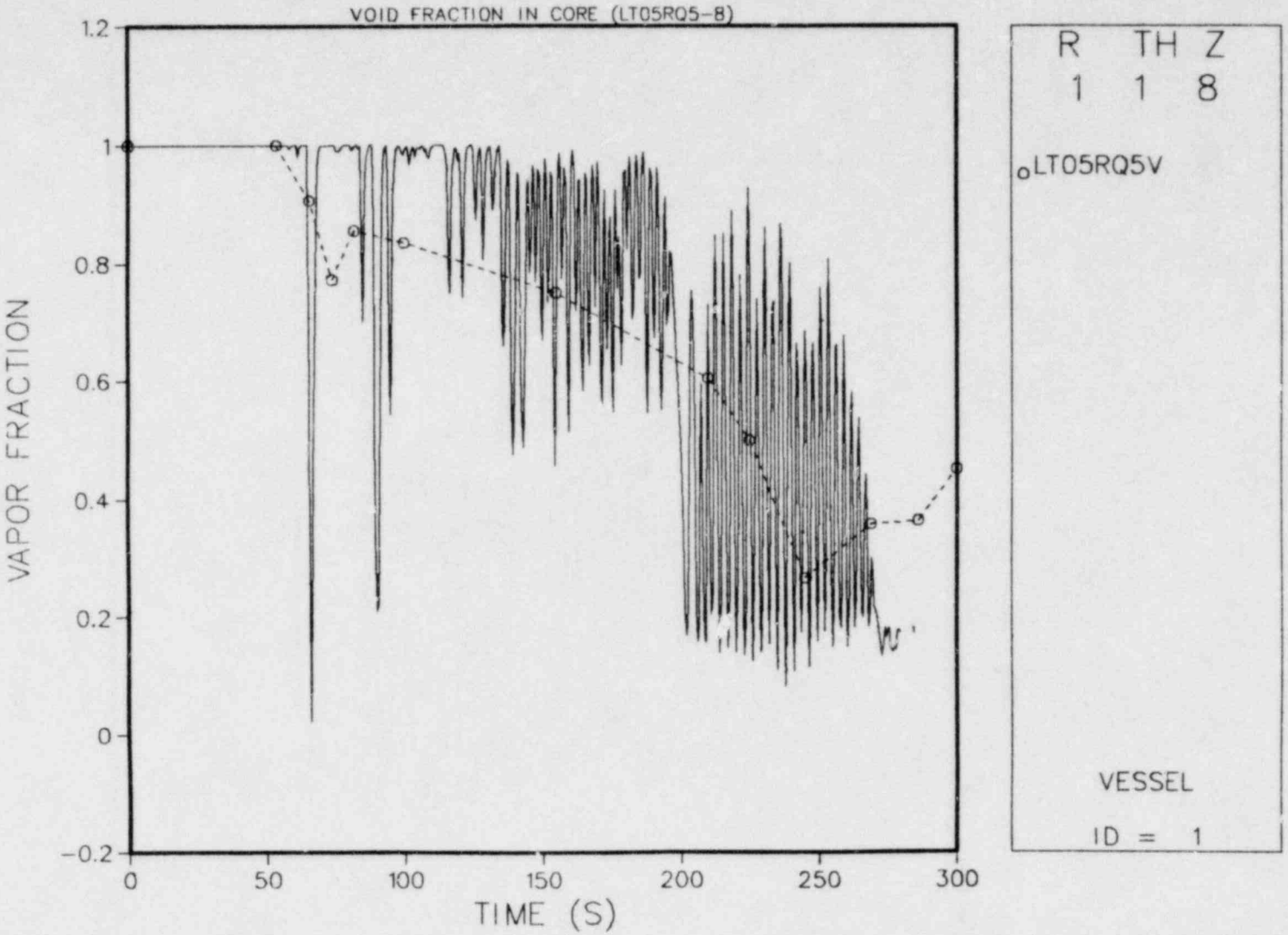

Fig. 14. Void fraction in core (Level 8).

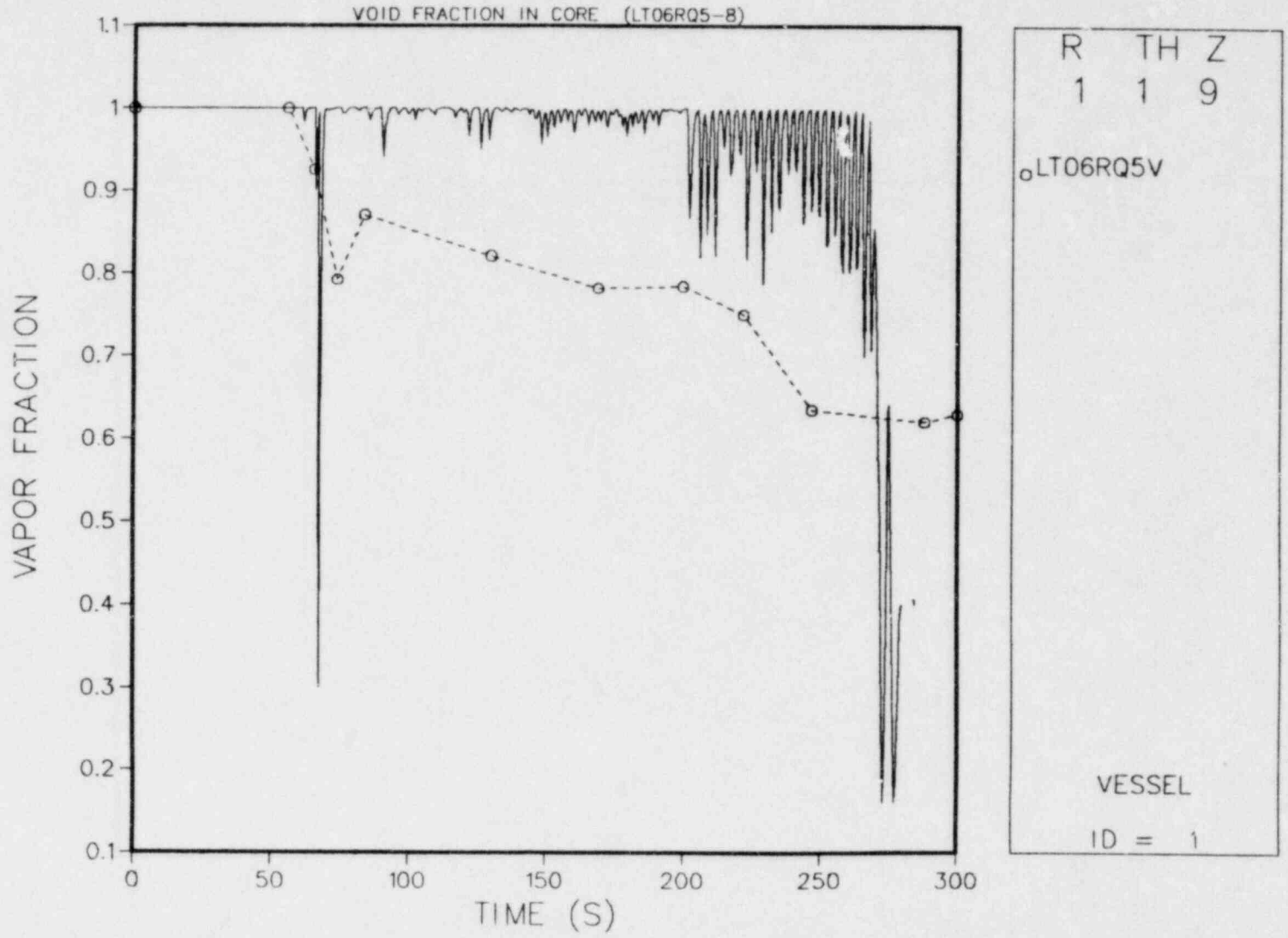

Fig. 15. Void fraction in core (Level 9).

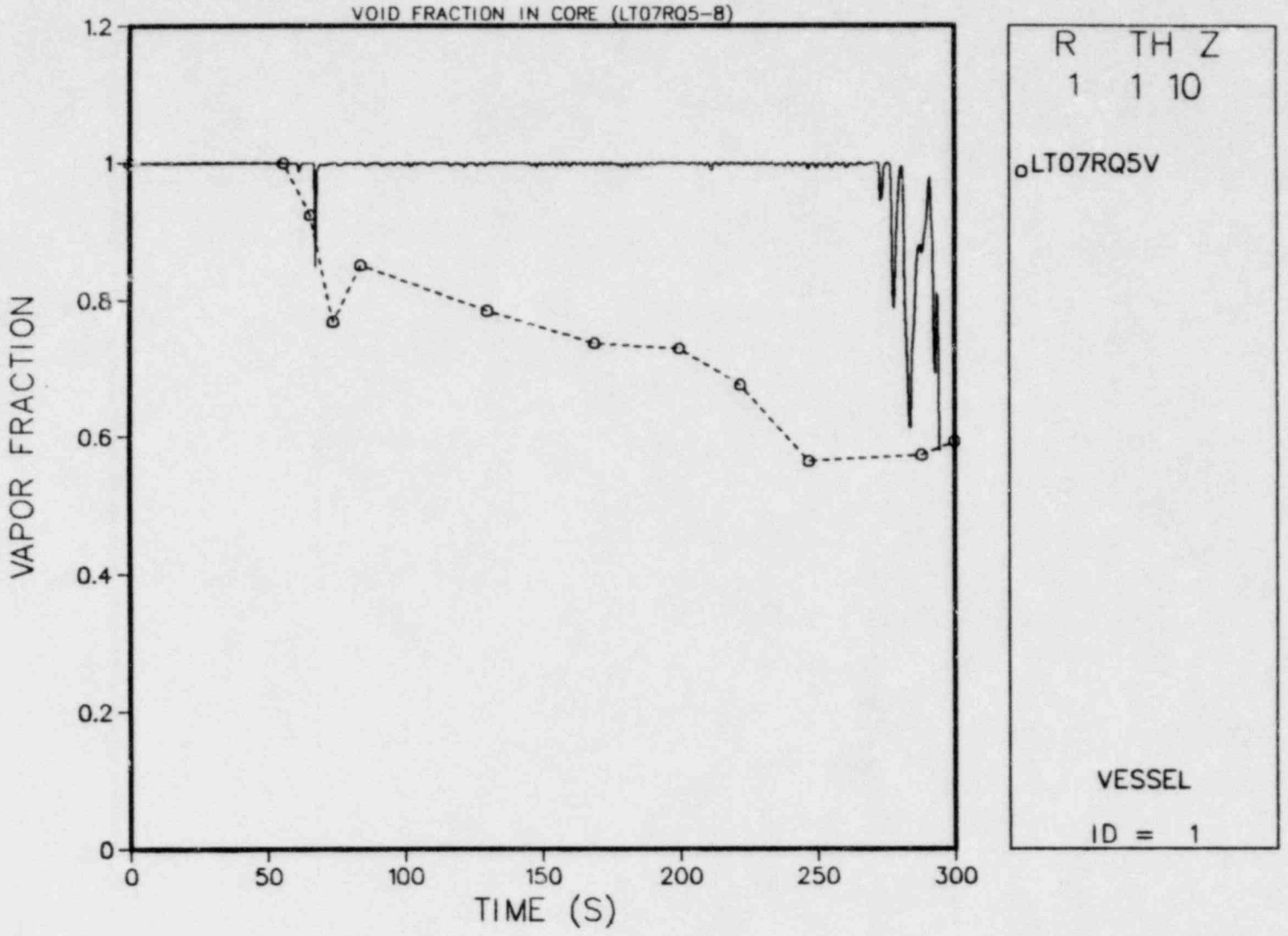

Fig. 16. Void fraction in core (Level 10).

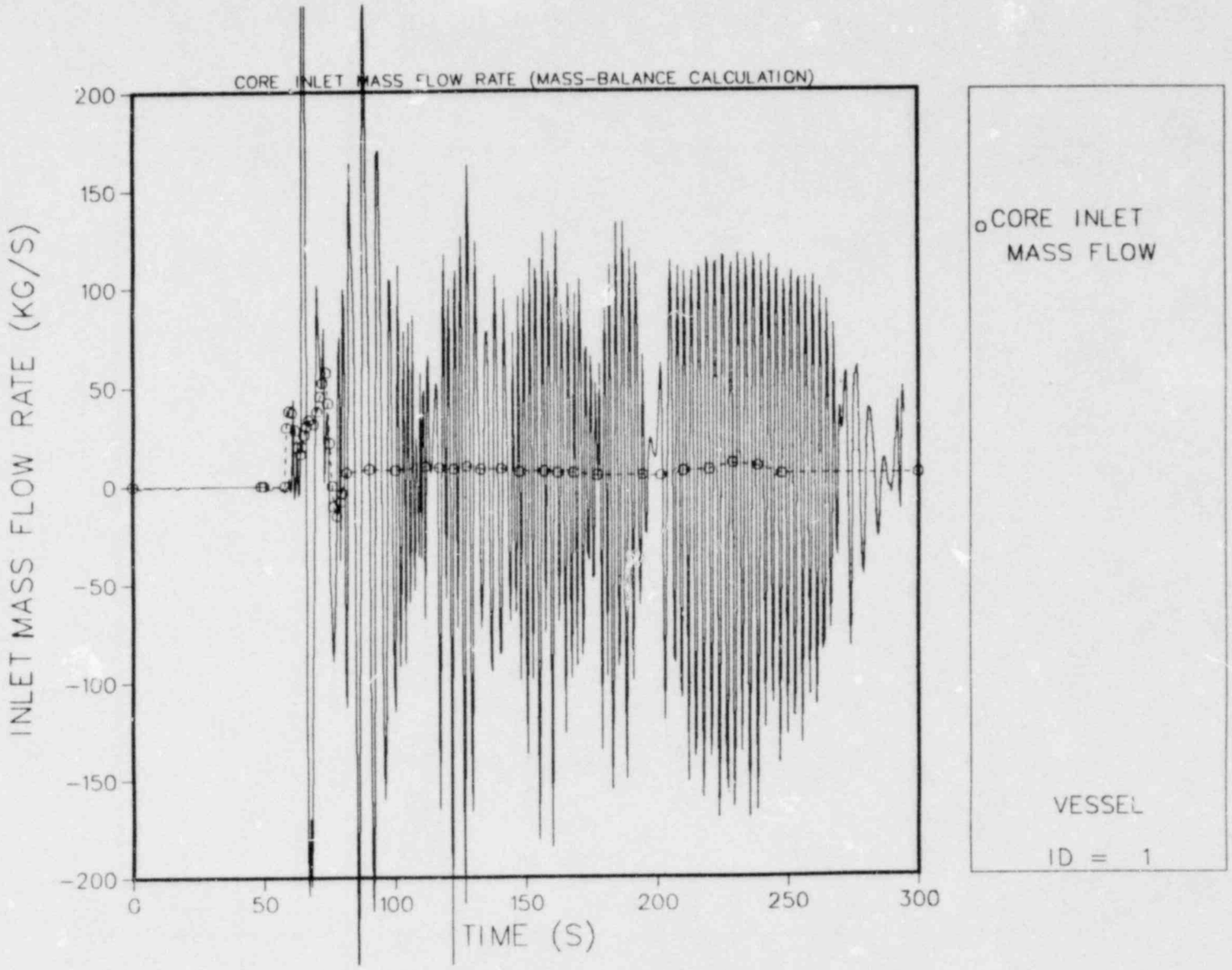

Fig. 17. Core inlet mass flow rate.

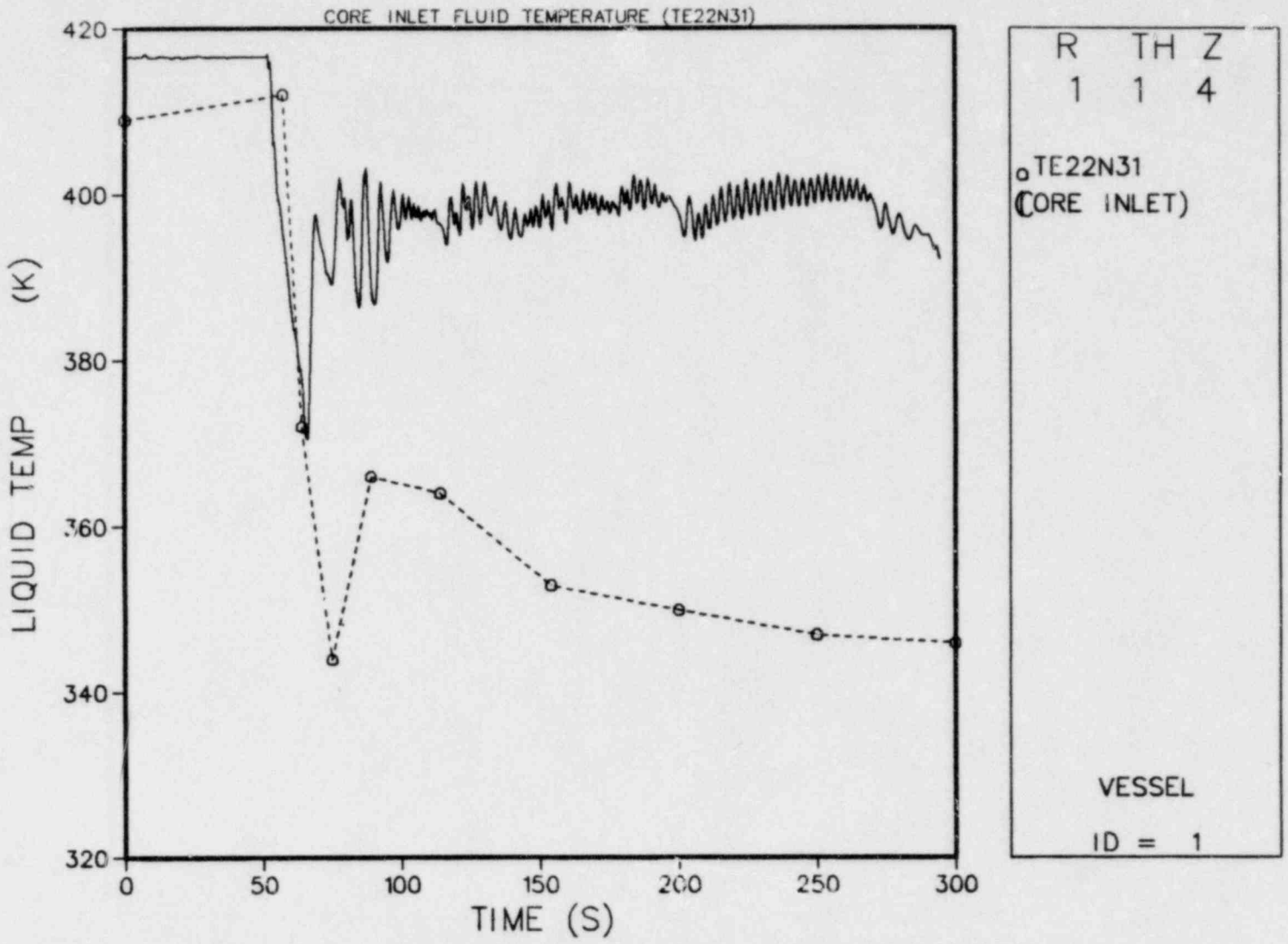

Fig. 18. Core inlet liquid temperature.

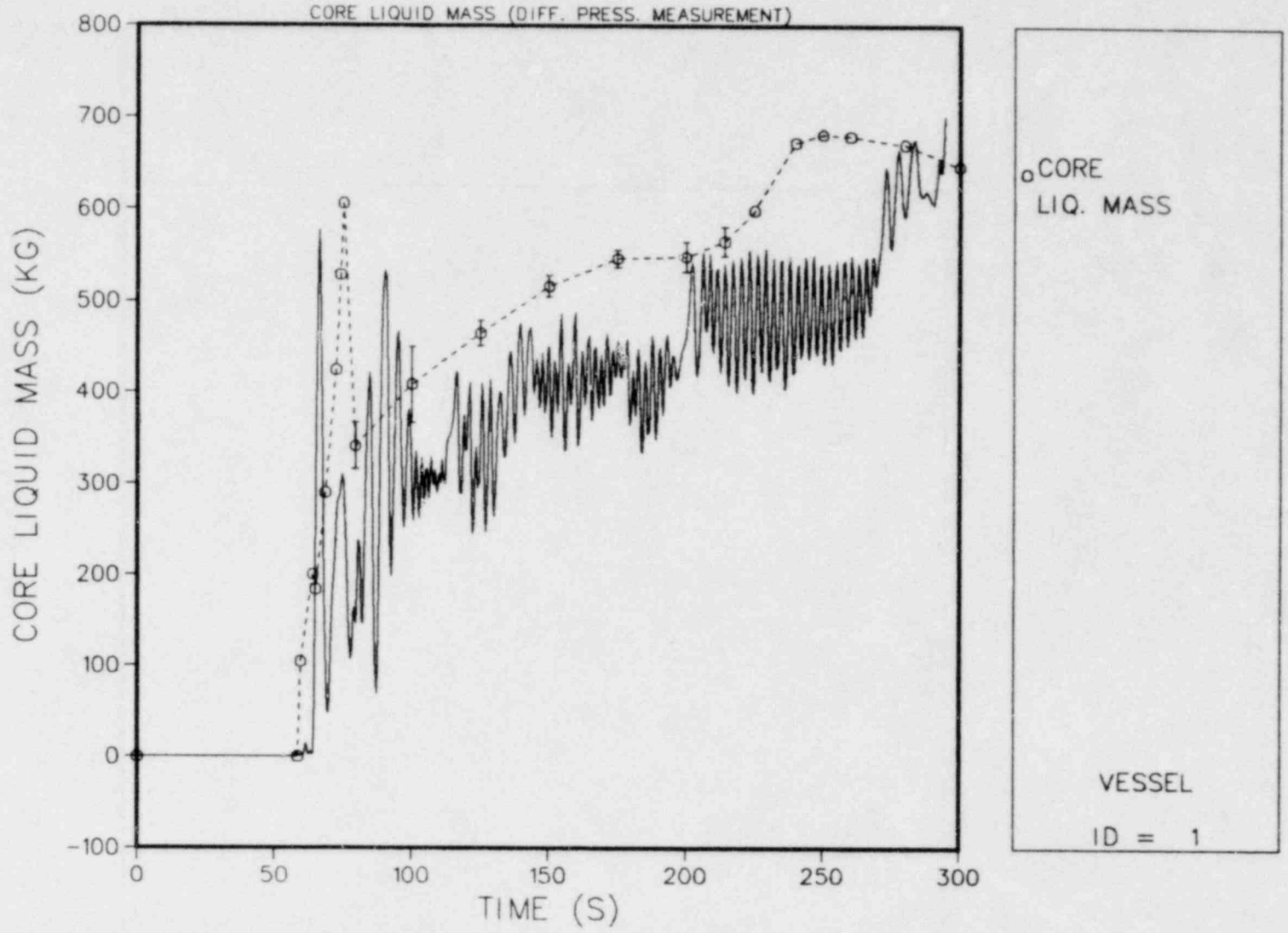

Fig. 19. Core liquid mass.

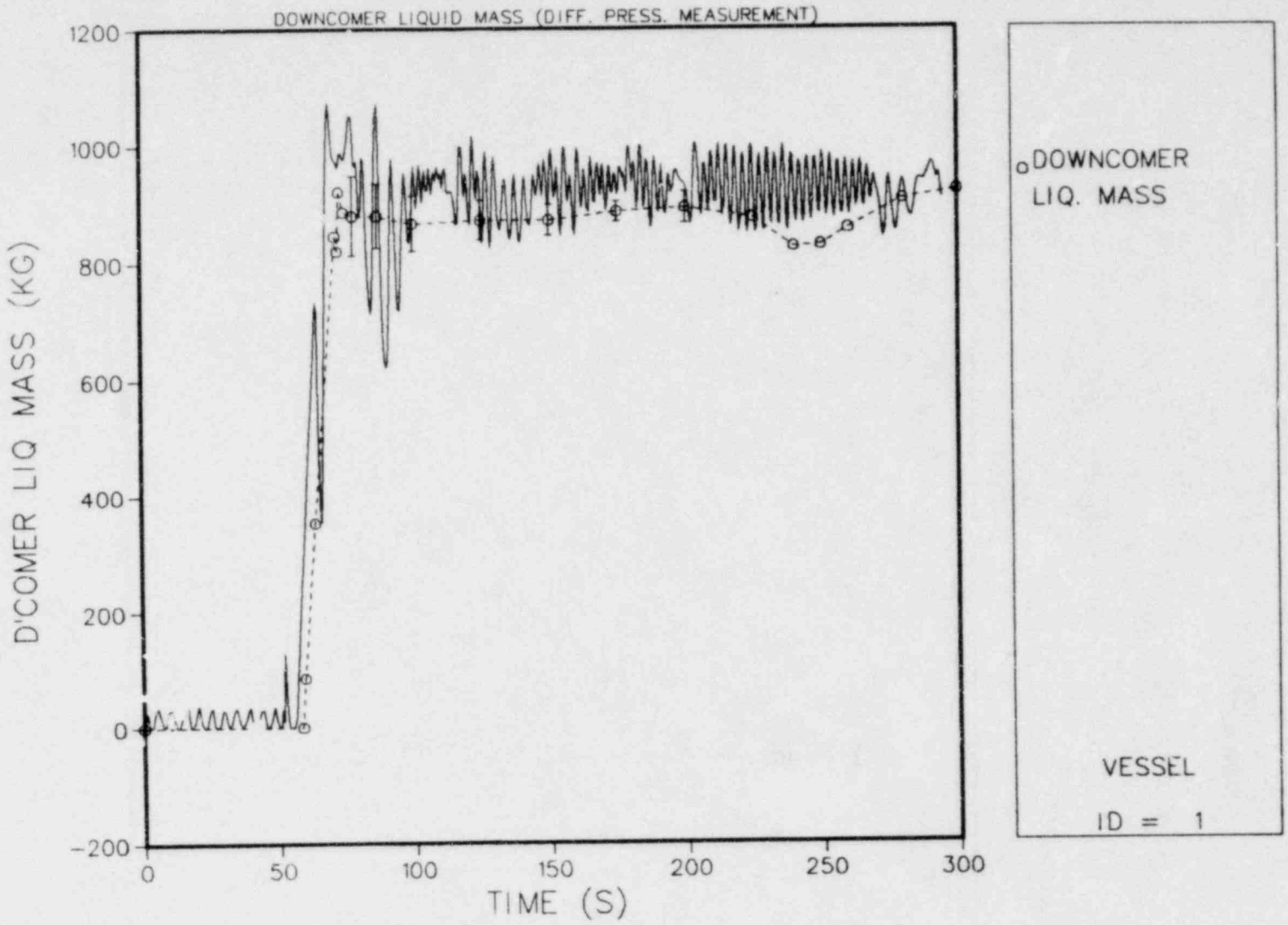

Fig. 20. Downcomer liquid mass.

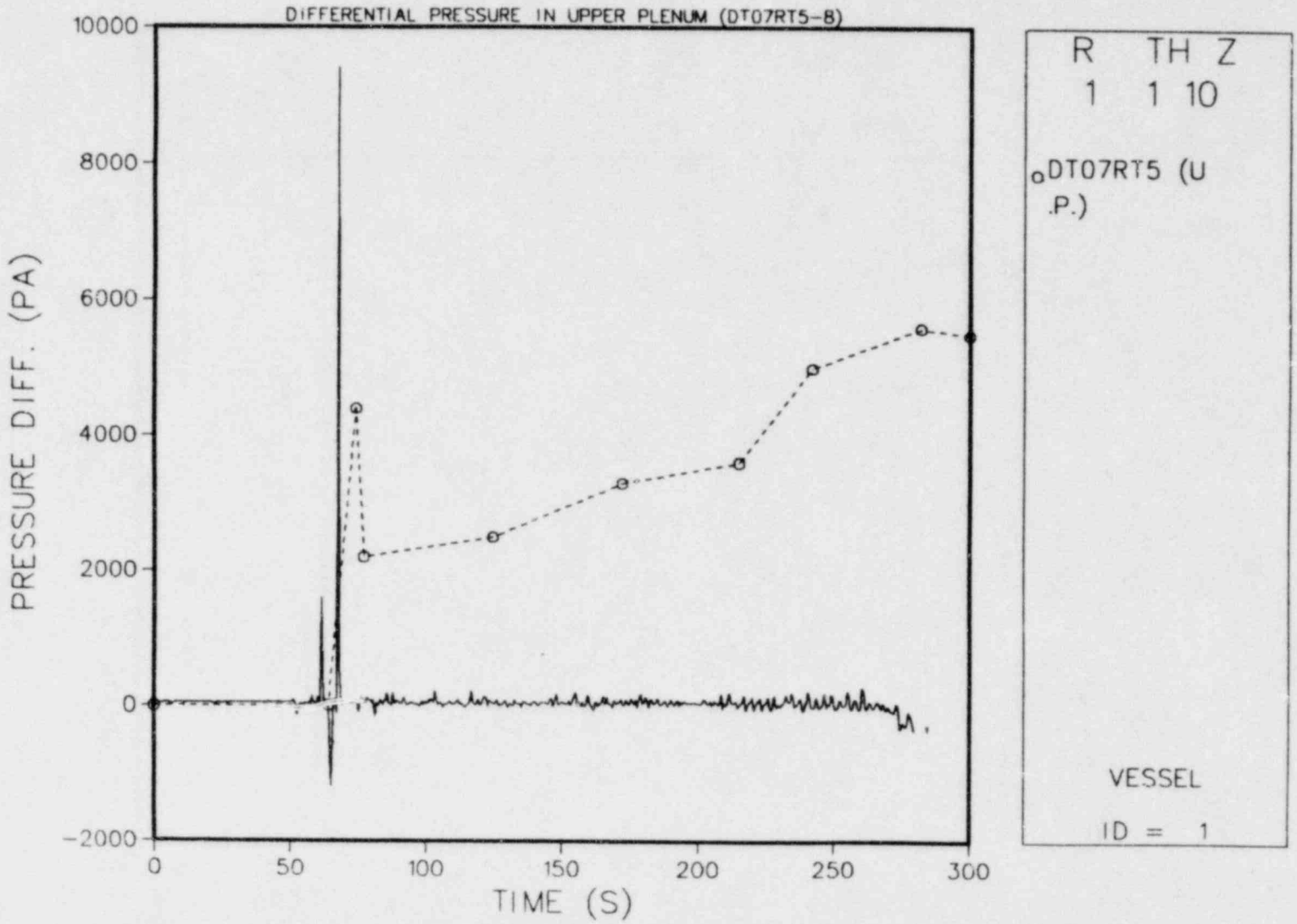

Fig. 21. Differential pressure in upper plenum.

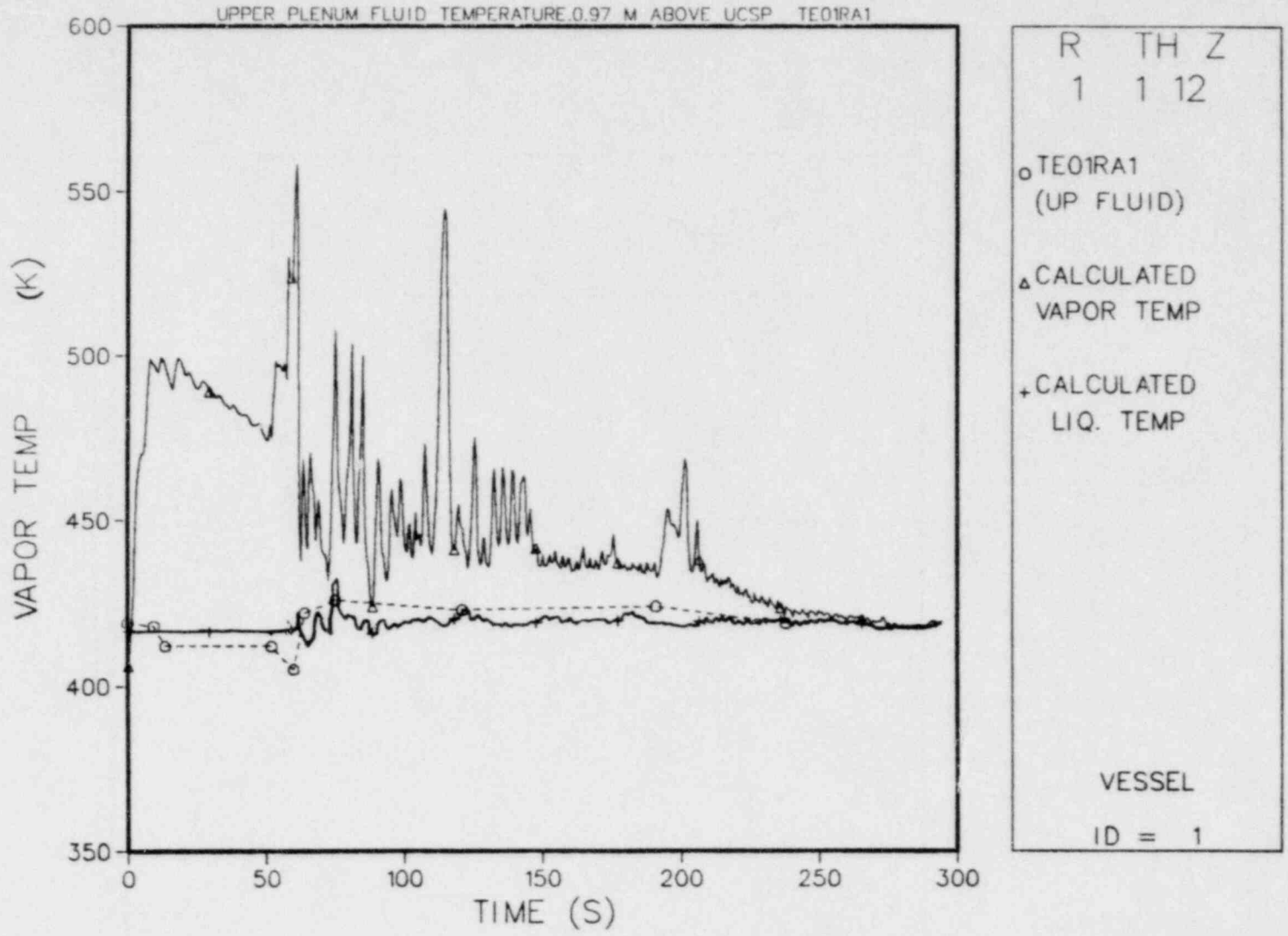

Fig. 22. Fluid temperature in upper plenum.

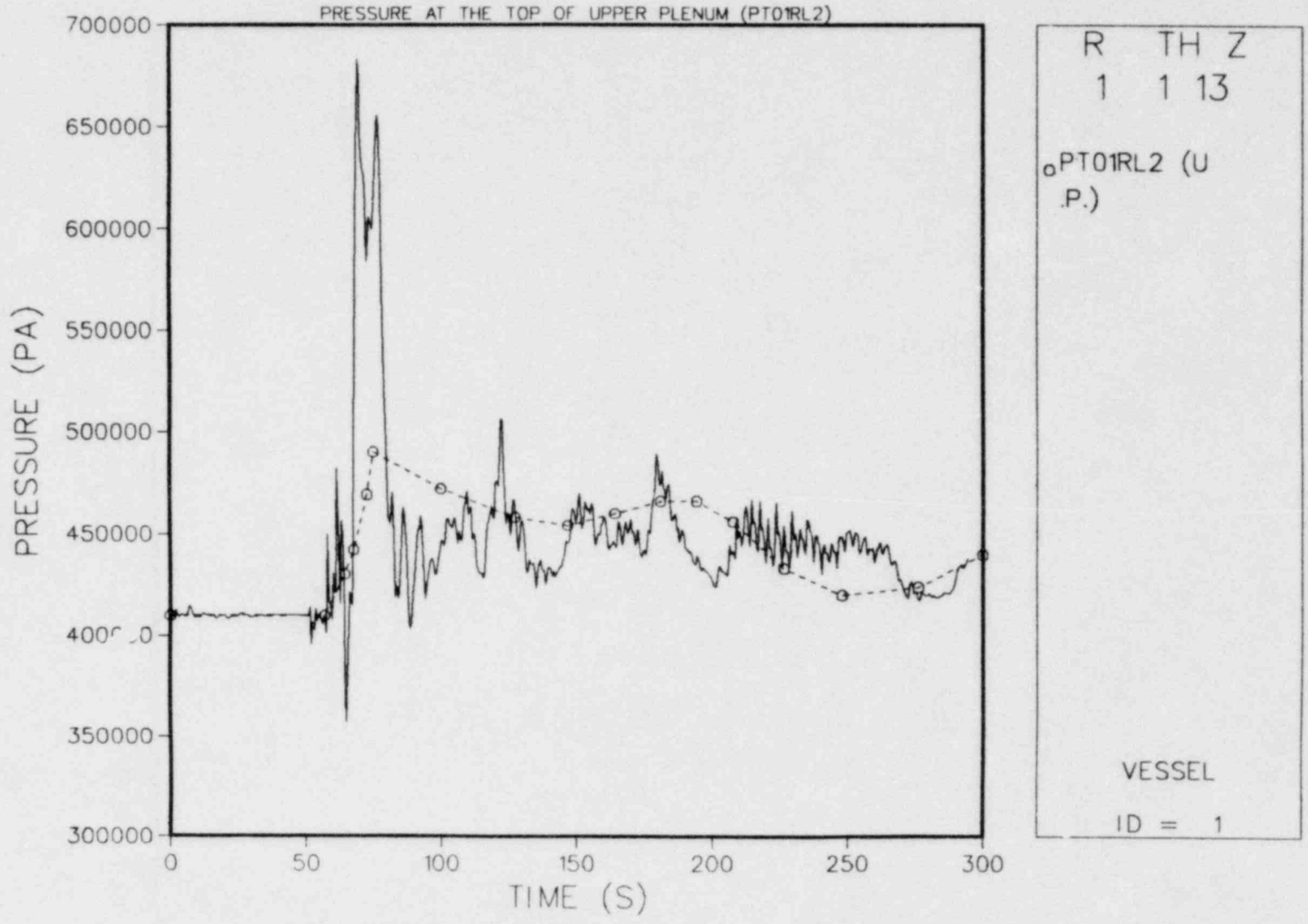

Fig. 23. Pressure in upper plenum.

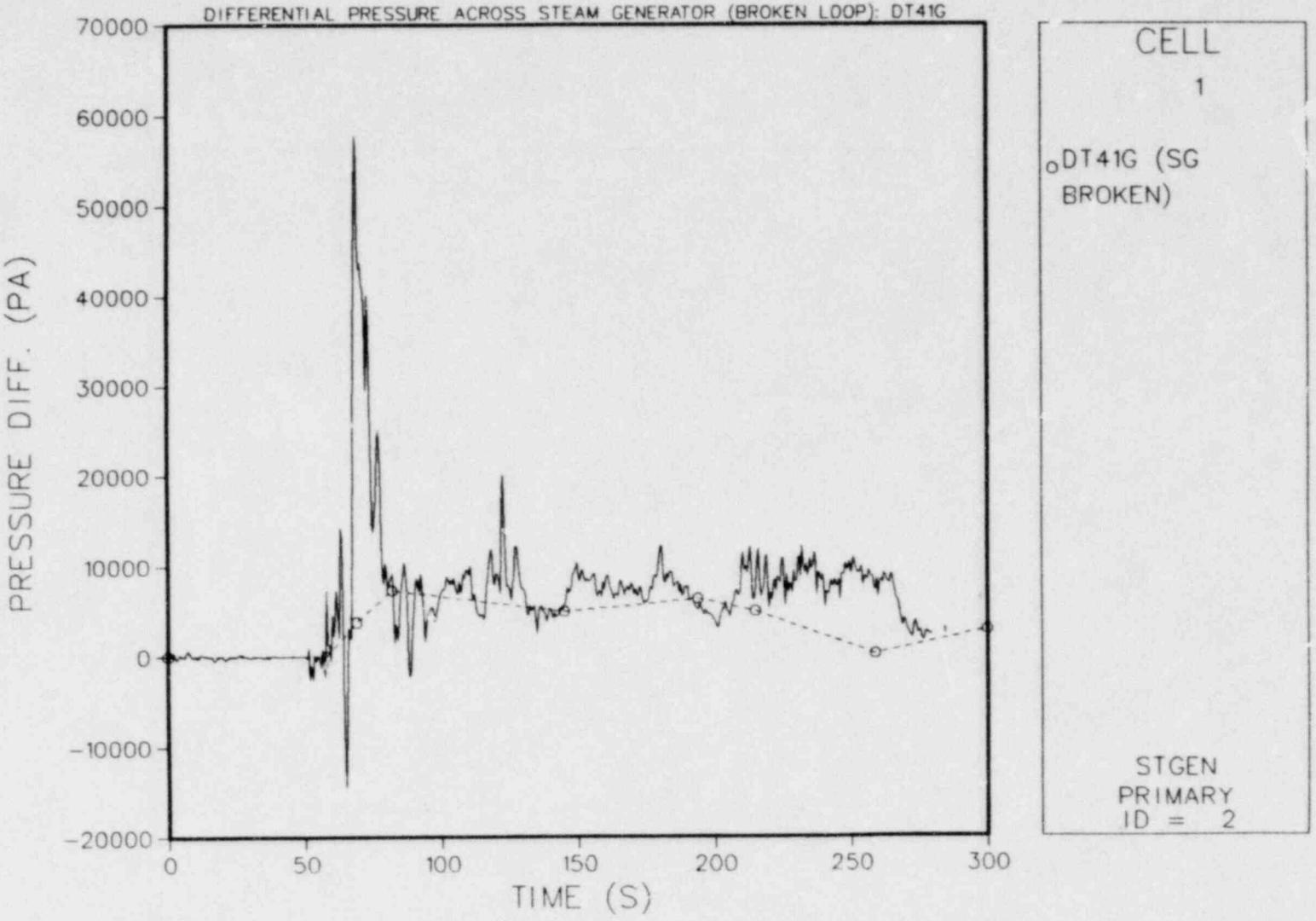

Fig. 24. Differential pressure across broken loop steam generator.

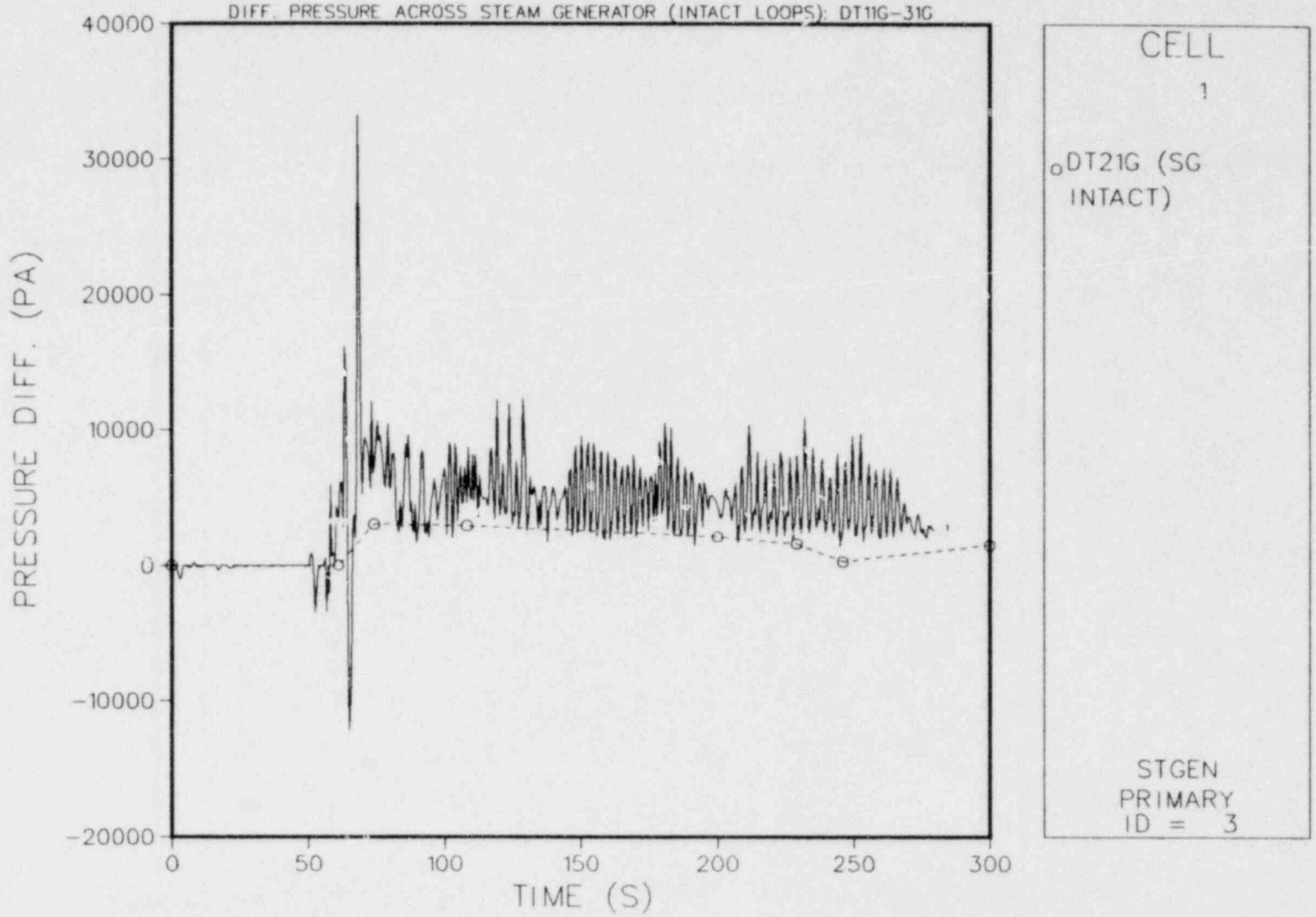

Fig. 25. Differential pressure across intact loop steam generator.

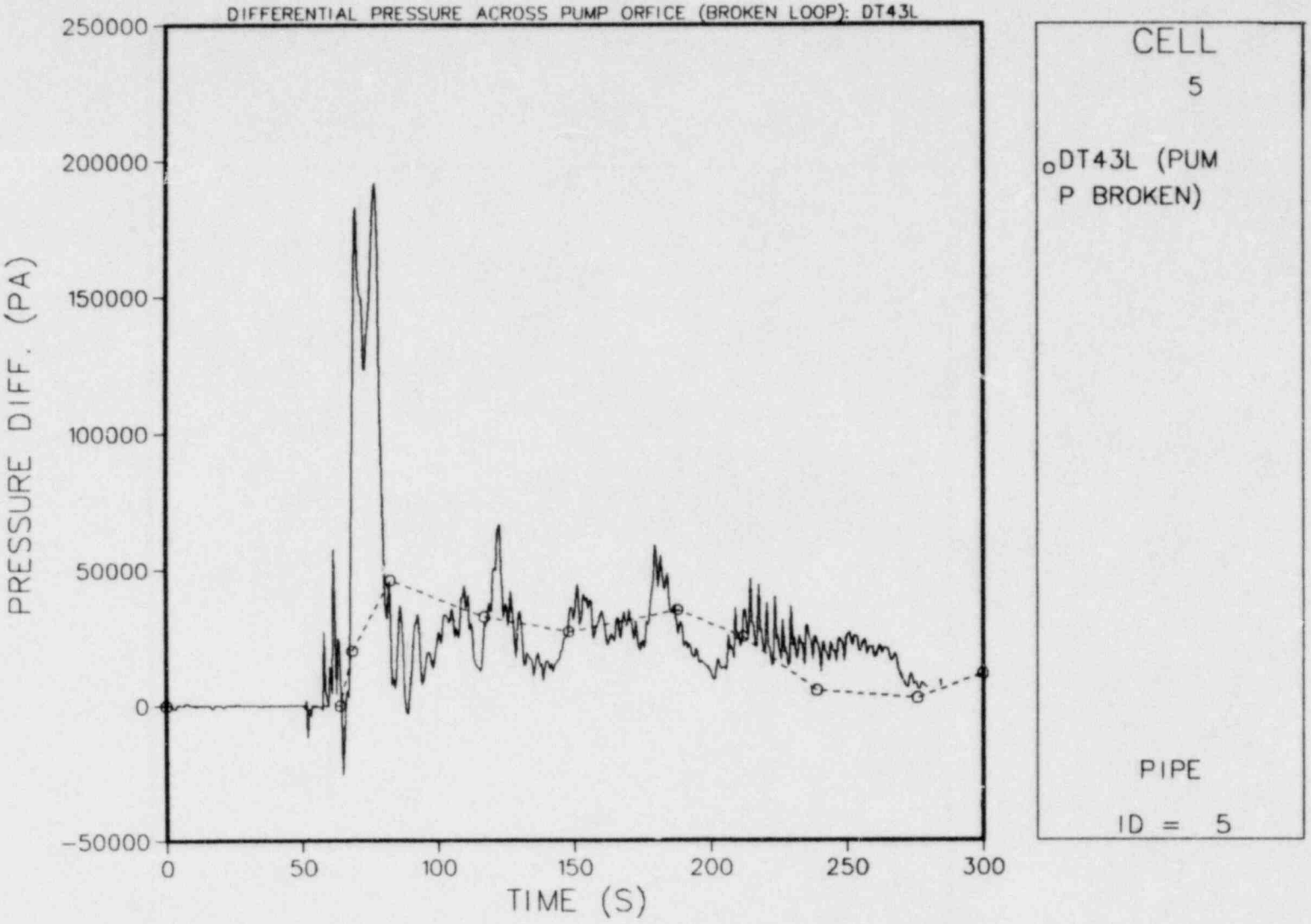

Fig. 26. Differential pressure across broken loop pump simulator.

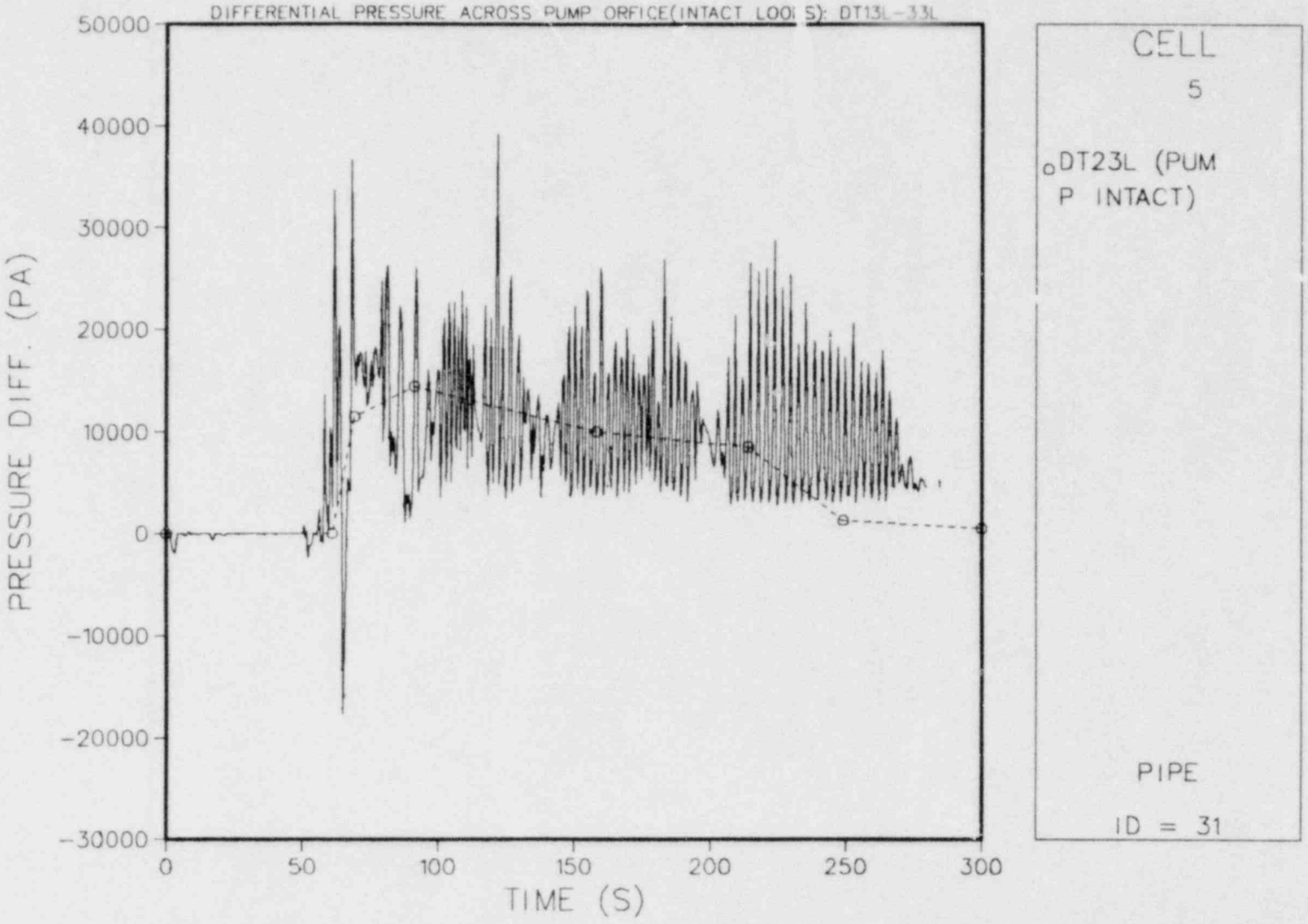

Fig. 27. Differential pressure across intact loop pump simulator.

TABLE I

SYSTEM MODEL COMPONENTS

Component Number	Component Type	Description	Cells
1	Vessel	Vessel: 2 radial rings, 2 azimuthal segments, and 13 axial levels; core located in ring 1, levels 5 through 10; piping connections in levels 1 and 12	52
2	STGEN	Broken loop steam generator	8,3
3	STGEN	Intact loop steam generator	8,3
4	PIPE	Broken loop hot leg	3
5	PIPE	Broken loop loop seal and pump	6
6	PIPE	Broken loop cold leg	3
7	BREAK	Containment 2 back pressure	1
8	BREAK	Containment 2 back pressure	1
9	FILL	ECC injection port	1
10	TEE	Intact loop cold leg	2,1
11	PIPE	Intact loop hot leg	3
12	FILL	Broken loop steam generator secondary feed water	1
13	FILL	Broken loop steam generator secondary feed water	1
14	FILL	Intact loop steam generator secondary feed water	1
15	FILL	Intact loop steam generator secondary feed water	1
16	FILL	Lower plenum injection port	1
17	VALVE	Lower plenum injection nozzle	3
31	PIPE	Intact loop loop seal and pump	6

TABLE II

INITIAL CONDITIONS FOR TEST C1-16 (RUN 025)

	Measured	Calculation for TRAC
Power		
Total (MW) :	9.82	9.82
Linear (kW/m) :	1.5	1.5
Radial Power Distribution	1.06:1.0:0.79	Flat
Decay Type : 1.2xANS + Actinide (30 s after SCRAM)		
Pressure (Pa)		
System :	4.1×10^5	4.1×10^5
Steam Generator Secondary:	5.0×10^6	5.0×10^6
Temperature (K)		
Downcomer Wall :	410.2	410.2
Primary Piping Wall :	418.2	418.2
Steam Generator Secondary :	536.2	536.2
Peak Clad at ECC Initiation :	801.2*	756.0**
Peak Clad at BOCREC :	866.2*	802.7**
Lower Plenum Filled Liquid:	400.2	400.2
ECC Liquid :	340.2	340.2
Water Level (m)		
Lower Plenum :	0.9	0.90
Steam Generator Secondary:	7.4	7.4
ECC Injection Rate (m^3/h)		
Accumulator :	361	361
LPCI :	40.1	40.1

*Measured at highest power rod in highest power region.

**Calculated at average power rod in medium power region.

TABLE III

SEQUENCE OF EVENTS FOR CCTF TEST C1-16 (RUN 025)

Event	Measured (s)	Calculated (s)
Test Initiated (Heater Rod Power Turned On)	0.0	0.0
Accumulator Injection Initiated (Lower Plenum)	49.0	49.0
Power Decay Initiated (Bottom of Core Recovery)	58.0	58.0
Downcomer Water Level Reaches Maximum Value	73.0	68.0
Accumulator Injection Ended and LPIS Initiated (Lower Plenum)	75.0	75.0
Time to Reach Peak Rod Surface Temperature at Core Midplane (22Y Rod)	70.0	83.5
All Heater Rods Quenched	268.0	272.0

DISTRIBUTION

	Copies
Nuclear Regulatory Commission, R4, Bethesda, Maryland	388
Technical Information Center, Oak Ridge, Tennessee	2
Los Alamos National Laboratory, Los Alamos, New Mexico	50
	440

Available from

GPO Sales Program
Division of Technical Information and Document Control
US Nuclear Regulatory Commission
Washington, DC 20555

and

National Technical Information Service
Springfield, VA 22161